Electronic Supplementary Material (ESI) for Chemical Science.

Supporting information

A Dynamic Cascade DNA Nanocomplex to Synergistically Disrupt Pyroptosis Checkpoint and Relieve Tumor Hypoxia for Efficient Pyroptosis Cancer Therapy

Xiaoni Wang[1], Xiyang Ge[1], Min Zhang[1], Jianghui Sun[1], Jin Ouyang[2] and Na Na*[1]

1 Key Laboratory of Radiopharmaceuticals, Ministry of Education, College of Chemistry, Beijing Normal University, Beijing 100875, China.

E-mail: nana@bnu.edu.cn

2 Department of Chemistry, College of Arts and Sciences, Beijing Normal University at Zhuhai, Zhuhai City, Guangdong Province 519087, China.

Table of Contents

Experimental Procedures

Chemicals and materials

All the DNA oligonucleotides (purified by HPLC) were customized from Sangong Biotech. Sequences of all oligonucleotides are listed in **Table S1**. 5,10,15,20-Tetrakis-(N-methyl-4-pyridyl)-porphine (TMPyP4), 3,3',5,5'-tetramethyl-benzidine (TMB) of analytical reagent grade were obtained from Aladdin Biochemical Technology Co., Ltd. (Shanghai, China). Glutathione reduced (GSH), titanic sulfate ($Ti(SO_4)_2$), 1,3-Diphenylisobenzofuran (DPBF) were obtained from Aladdin Reagent, Ltd. (Shanghai, China). Sodium hydroxide (NaOH), and hydrogen peroxide (H_2O_2, 30%) were obtained from Beijing Chemical Works (Beijing, China). 5,5' -dithiobis-2-(nitrobenzoicacid) (DTNB) and ethanol anhydrous were purchased from Sinopharm Chemical Reagent. Dulbecco's modified Eagle's medium (DMEM), trypsin and phosphate buffered saline (PBS, pH 7.4, basic (1×)) were acquired from Sigma-Aldrich. WB Transfer Buffer (10×), BCECF-AM intracellular ratiometric pH indicator, 2',7'-dichloro fluorescein diacetate (DCFH-DA), acridine orange (AO), qPCR-related reagents, ATP Assay Kit, Lactate dehydrogenase (LDH) cytotoxicity assay kit, LC3B Antibody (Rabbit Polyclonal Antibody), 2',7'-bis-(2-carboxyethyl)-5-(and-6)-carboxyfluorescein acetoxymethyl ester (BCECF-AM), Annexin V-FITC/PI apoptosis detection kit, mitochondrial membrane potential assay kit, Reactive Oxygen Species Assay Kit were purchased from Solarbio Science & Technology. GSH assay kit and lactate assay kit were purchased from Beyotime (China). Calcein-AM, LysoTracker Green was purchased from Thermo Fisher Scientific Inc. (Shanghai, China). 3-(4,5-dimethylthiazol-2-yl)-2,5-diphenyltetrazolium bromide (MTT) solution, DNA ladder, Hoechst 33342 staining solution and Liperfluo (LPO) were purchased from Sangon Biotech Co., Ltd. (Shanghai, China). Ultrapure water (Mill-Q, Millipore, 18.2 MΩ) was used in all experiments. All chemicals were used without further purification. The female BALB/c nude mice (5 weeks, 18-20 g) used for animal experiments were provided by Beijing Vital River Laboratories (China).

Instruments

The transmission electron microscopy (TEM) images were obtained with a FEI Talos F200s TEM (Thermo Fisher Scientific, USA). Ultraviolet-visible (UV-vis) spectra were acquired using a Shimadzu UV-2600 spectrophotometer (Shimadzu, Japan). The fluorescence spectra were recorded on an FS5 fluorescence spectrometer (Edinburgh, UK). The dynamic light scattering (DLS) and zeta potential data were conducted using the Nano-ZS Zetasizer ZEN3600 (Malvern, UK.). The cell viability was measured by thiazolyl blue tetrazolium bromide (MTT) using a microplate reader at 490 nm on a microplate reader (BioTek, USA). Confocal fluorescence imaging of cells was performed on a Nikon A1R-si laser confocal laser scanning microscope (CLSM) (Nikon, Japan). Flow cytometric analysis was performed on CytoFLEX (Beckman, USA). Tissue slides images were captured using a Zeiss Axiovert 20 inverted fluorescence microscope (Carl Zeiss, Germany). *In vivo* imaging was performed on an IVIS Lumina III system (Caliper, USA).

Methods

Synthesis of ZnO_2 NPs: ZnO_2 NPs were fabricated following a simple and green wet chemistry approach with modification.[1] Briefly, 0.1 g of $Zn(OAc)_2$ and 0.1 g of PVP were dissolved in 5.0 mL of deionized (DI) water. Then, 0.5 mL of H_2O_2 was quickly added under a vigorous stirring. After reaction for 24 h, the unreacted residue was removed by centrifugation at 15,000 rpm for 15 min and rinsing three times with DI water. The final PVP-modified ZnO_2 NPs were re-dispersed in ethanol (95%) and used for the synthesis of ZnO_2-Mn NPs. Then a solution of 10 mg $KMnO_4$ in 1 mL MQ was added dropwise under ultrasonication. The mixture was sonicated for 10 min. After being centrifugated (10000 g, 10 min) and washed with Milli-Q water for 2 times, ZnO_2-Mn NPs was obtained and redispersed in MQ for further use.

Synthesis of DNFs: Rolling circle amplification (RCA) reaction was used to prepare the programmed DNFs. 5'-phosphorylated linear template (2 μM) and primer (2 μM) were hybridized in 100 μL water by heating at 95°C for 5 min, followed by gradual cooling to room temperature over 1 h. The annealed product (1 μM) was chemically connected by adding 2 μL of T4 DNA ligase (40 U/μL) at 16°C for 4 h. The enzyme was deactivated by heating at 65°C for 10 min. Each RCA reaction was conducted in a final volume of

100 μL consisting of circularized template-primer complex (300 nM), dNTPs (1 mM), and phi29 DNA polymerase (1 U/μL) in DNA polymerization reaction buffer (33 mM Tris-acetate pH~7.9, 10 mM Mg-acetate, 66 mM K-acetate, 0.1% Tween 20, 1 mM dithiothreitol). Cy5-dCTP (10 μM) was introduced to the RCA reaction mixtures to prepare DNFs for fluorescence imaging.

Synthesis of DNA nanocomplex (DNFs@ZnMn): The RCA reaction was performed at 30°C for 4 h and stopped by inactivating polymerase at 75°C for 10 min. DNFs@ZnMn were synthesized by adding extra different concentration of ZnO_2-Mn in the RCA mixture. The resultant products were washed with water and centrifuged at 13,525 rcf for 5 min twice and then were sonicated to redisperse the DNFs@ZnMn. The obtained DNFs@ZnMn were redispersed in 100 μL PBS and kept at 4°C.

Study of the stability of DNFs: For the stability test, DNFs or DNFs@ZnMn was added into 10% fetal bovine serum (FBS), PBS and water incubated at 37°C for 0, 4, 6, 8, 12, 24 and 48 h, respectively. For the acid-base stability test, DNFs or DNFs@ZnMn was preincubated at different buffers (pH~5.5 and 7.4). Then these samples were verified by using 2% agarose gel electrophoresis stained with EB solution, visualized by UV illumination (302 nm), and photographed by a gel imaging analysis system (JS-680B).

Disparity of mRNA cleavage efficiency of different metal ions: Gel electrophoresis assay was performed to investigate the DNAzyme-affinity of different metal ions for initiating mRNA cleavage reaction. DNAzyme (400 nM) and substrate RNA (2 μM) was mixed and incubated for 1 h (37°C), and then different concentrations of metal ions were added to the mixture solution and incubated for another 1 h (37°C). In addition, the affinity of DNAzyme with ions was verified by different metal ions at the same concentration. Then the samples were diluted with 6×DNA loading buffer and loaded into a freshly prepared 3% native polyacrylamide gel. Electrophoresis was performed at a constant potential of 120 V in TBE buffer (89 mM Tris, 89 mM boric acid, 2.0 mM EDTA, pH~8.3) for 0.5 h. The bands were stained with ethidium bromide (EB), visualized by UV illumination (302 nm), and photographed by a gel imaging analysis system (JS-680B).

Examinations on the Specificity of metal ion as cofactors for mRNA cleavage: Gel electrophoresis assay was performed to investigate the DNAzyme mediated mRNA cleavage reaction. DNAzyme (400 nM) and substrate RNA (2 μM) was mixed and incubated for 1 h (37°C) and then different concentrations of metal ions (such as Mn^{2+}, Zn^{2+}) were added to the mixture solution and incubated for another 1 h (37°C). Then the samples were diluted with 6×DNA loading buffer and loaded into the freshly prepared 3% native polyacrylamide gel. Electrophoresis was performed at a constant potential of 120 V in TBE buffer (89 mM Tris, 89 mM boric acid, 2.0 mM EDTA, pH~8.3) for 0.5 h. The bands were stained with ethidium bromide (EB), visualized by UV illumination (302 nm), and photographed by a gel imaging analysis system (JS-680B).

Zn^{2+}-responsive self-sustained DNFs for programmable gene release: DNFs-n1@ZnMn, DNFs-n2@ZnMn, and DNFs@ZnMn were preincubated in acetate buffer (pH~5.0) for 1 h. Then, the buffer was adjusted to 10 mM Tris-HCl (pH~7.4, 100 mM NaCl) and incubated for 2 h. For kinetic analysis, these DNFs reactions were stopped by adding 95% formamide (20 mM EDTA). The self-cleavage reaction of DNFs was initiated by different concentrations of Zn^{2+} (0, 0.5, 1, 2, 3 and 4 mM) at 37°C. Denaturing PAGE characterization of DNAzyme-mediated DNFs cleavage was performed in Tris-HCl buffer (10 mM, pH~7.4, 100 mM NaCl) containing 0.5 mM Zn^{2+}, after incubating for different times (2, 4, 8 12 and 24 h). Each DNA sample (8 μL) was mixed with 6x loading buffer (1.6 μL) and analyzed using 12% polyacrylamide gel at 120 V for 30 min in 1x TBE buffer. The bands were stained with ethidium bromide (EB), visualized by UV illumination (302 nm), and photographed by a gel imaging analysis system (JS-680B).

pH-responsive release of Mn^{2+}, Zn^{2+} from ZnO_2-Mn: To detect the acid-induced release of Mn^{2+} and Zn^{2+}, the ZnO_2-Mn was dialyzed against the buffer at a specified pH (7.4, 6.5, 5.5). The dialysates were collected at predetermined times and the released Mn^{2+} and Zn^{2+} were detected by inductively coupled plasma mass spectrometry (ICP-MS).

GSH Depletion: PBS, DNFs, ZnO_2, ZnO_2-Mn and DNFs@ZnMn (2 mg/mL) were mixed

with GSH aqueous solution (10 mM), followed by adding 0.2 mM of DTNB to detect the –SH group in GSH for 24 h. The absorbance changes at 412 nm were recorded by a UV-vis spectrophotometer.

H_2O_2 generation: $Ti(SO_4)_2$ was used as a H_2O_2 indicator whose color changed from colorless to yellow when specifically reacting with H_2O_2. 1 mg DNFs@ZnMn was dispersed in 1 mL of solutions at different pH values (7.4, 6.8, 6.5, 6.0 and 5.5), and the mixture was stirred for 1 min. Next, the supernates were collected by centrifugation and mixed with 1 mL of $Ti(SO_4)_2$ solution (1 mg/mL). After that, the absorbances were recorded using a UV-vis spectrophotometer.

Oxygen generation: In order to verify the effect of H_2O_2 concentration on the O_2 production capacity of materials. Four milligrams of DNFs@ZnMn or DNFs was incubated with 10 mL of different pH solution at 37°C. To examine the O_2 production capacity of different materials, PBS, DNFs, and DNFs@ZnMn (the concentration of ZnO_2-Mn and DNFs was 100 μg/mL) was mixed in 10 mL of PBS at room temperature. In addition, to investigate the influence of acidic condition on the O_2 generation, the DNFs@ZnMn was also dispersed in different pH (5.5, 6.5 and 7.4) buffer. The dissolved O_2 concentrations were real-time monitored by a dissolved oxygen meter (JPSJ-605F Dissolved Oxygen Meters)

$^1O_2$ Generation During NIR Light Irradiation: The highly selective $^1O_2$ probe of SOSG was selected for evaluating $^1O_2$. In brief, 100 μL of SOSG (0.1 mM) solution was mixed with 2 mL of different nanomaterials solutions. Then, the mixture was exposed to NIR laser (660 nm, 0.2 W cm^{-2}) at fixed time intervals.

The Fenton catalytic performance of the different nanoparticles was monitored through a TMB color test. Briefly, 100 μL DNFs@ZnMn suspensions (200 μg·mL^{-1}) were immigrated in a solution containing phosphate-buffered saline at different pH values, TMB (dissolved in DMSO, 1 mg/mL, 200 μL), and H_2O_2 (30 μL, 30%). After 5 min, the mixture was subjected to the absorption spectrum analysis (λ = 660 nm) via a UV-Vis spectrometer.

Photocatalytic and Chemodynamic Degradation of DPBF: The 1,3-

diphenylisobenzofuran (DPBF) probe was used to evaluate the ROS production ability of DNFs@ZnMn. Generally, 30 μL DPBF (10 mM) was added into 2 mL DNFs@ZnMn aqueous solution. Then mixed solution was irradiated by NIR laser with a power density of 0.2 $W \cdot cm^{-2}$ for 10 min. The absorption of supernatant was measured at different irradiation times. Moreover, the light triggered ROS generation ability of DNFs and PBS was also measured using DPBF probe under the same light condition.

Cell Culture under Hypoxia Condition: The HeLa cells, A549 cells, MCF-7 cells, HUVEC cells, HEK-293T cells, L02 cells line was cultured in DMEM culture medium supplemented with 1% (v/v) penicillin, 1% (v/v) streptomycin, and 10% (v/v) fetal bovine serum at 37°C using a modular incubator chamber containing 94% N_2, 1% O_2 and 5% CO_2 (to simulate the anoxic gas environment). After being seeded in plates, the cells were put in the modular incubator chamber and the above mixed gas was pumped into the chamber for 20~30 min. Then, the chamber was put in the normal incubator for the cell culture overnight.

Confocal Fluorescence Imaging: To investigate the cellular uptake efficiency of DNFs@ZnMn, HeLa cells, A549 cells, MCF-7 cells, HUVEC cells, HEK-293T cells, L02 cells line that seeded in 6-well plates (2×10^5 cells per well) were exposed to Cy5-labeled DNFs@ZnMn (100 μM) and Cy5-labeled DNFs for different times (0 h and 8 h). Then the cells were removed and washed with PBS for three times, the cells were digested by trypsin-EDTA solution with 0.25% phenol red and resuspended by PBS following by analysis with a flow cytometer (FACSAria III, BD, USA).

Colocalization analysis: The lysosome escape analysis was characterized by confocal imaging. Specifically, HeLa cells were incubated with Cy5-labeled DNFs@ZnMn for 8 h in confocal cell culture dishes. After washing twice with PBS, the cells were irradiated with near-infrared laser (660 nm) for 10 min. Then 5×10^{-6} M Lyso-Tracker Green was added and incubated with cells for another 30 min. Cell nuclei were stained by Hoechst for 20 min. After washing with cold PBS twice, the cells were immediately observed by CLSM.

Investigation of endocytosis pathway: HeLa cells were seeded in a 35 mm cell culture

dish (2 × 10^5 cells per well) and cultured for 12 h. Next, the cells were pre-incubated with several inhibitors that were specific via different endocytosis pathways for 60 min at 37°C, including chlorpromazine hydrochloride (10 μg/mL) for clathrin-mediated endocytosis, genistein (200 μg/mL) for pit mediated endocytosis, Me-β-CD (500 μM) for lipid-raft mediated endocytosis, amiloride (2 mM) for macro-pinocytosis mediated endocytosis, nystatin (1 mM) for caveolin-mediated endocytosis, and wortmannin (400 nM) for macropinocytosis. Afterwards, the cells pre-treated with the inhibitors were incubated with Cy5-labeled DNFs@ZnMn for 4 h at 37°C, whereas the cells untreated with inhibitors were incubated with Cy5-labeled DNFs@ZnMn for 4 h at 4°C and used for control experiment. Finally, the cells were fixed with 4% fixative solution for 20 min and washed twice with PBS, stained by Hoechst 33342 (5 μg/mL) for another 15 min using a standard procedure. Finally, the samples were imaged by CLSM. HeLa cells were seeded into 6-well culture plates and cultured at 37°C for 24 h. Next, the cells were pre-incubated with several inhibitors that were specific through different endocytosis pathways for 60 min at 37°C. Afterwards, the cells pre-treated with the inhibitors were incubated with Cy5-labeled DNFs@ZnMn for 4 h at 37°C. After incubation, the cells were washed with PBS, digested and resuspended in PBS. The uptake of the Cy5-labeled DNFs@ZnMn into cells was then analyzed with flow cytometer.

Tumor Sphere Culture and Observation: The HeLa multicellular spheroids (MCSs) were established by a liquid overlay method. Briefly, a 96-well spheroid microplate was coated with 1.5 % agarose gel to prevent cell adhesion. Then, the cell suspensions (2 × 10^5 cells / 200 μL per well) were transferred into each well, gently agitated for 5 min, and maintained at 37°C for 7 days. The uniform and complete spheroids were used for the penetration studies. The Cy5-labeled nanomaterials were incubated with the tumor spheroids at 37°C for 8 h. Then, the medium was removed and the spheroids were gently washed with PBS three times. The fluorescent signal of Cy5 in spheroids was observed using the Z-stack images of the confocal microscope.

Intracellular Zn^{2+} and Mn^{2+} detection: Zinquin ethyl ester, a cell-permeable

fluorescent probe for Zn^{2+} was used to detect the intracellular Zn^{2+} level. After incubation with PBS, DNFs, DNFs-n1@ZnMn DNFs-n2@ZnMn and DNFs@ZnMn for 8 h, the HeLa cells were stained with Zn^{2+} dye (5 μM) successively. Then, the fluorescence images were collected with the Nikon 80i epi-fluorescence microscope for Zn^{2+} dye. Afterwards, the cells pretreated with the inhibitors were incubated with DNFs@ZnMn (equal to 200 μg/mL of DNFs and ZnO_2-Mn) for 4 h at 37°C. After incubation, the cells were washed with PBS, digested and resuspended in PBS. The uptake of the DNFs@ZnMn into cells was then analyzed with flow cytometer.

To quantitatively detect the intracellular Mn^{2+} and Zn^{2+} level, HeLa cells incubated with DNFs@ZnMn NPs for 4 h were digested and treated with aqua regia. Quantitative analysis of Mn^{2+} and Zn^{2+} was carried out by ICP-MS. The contents of Mn^{2+} and Zn^{2+} in the cells was calculated as nanogram per 2×10^5 cells.

Intracellular O_2 levels measurement: Intracellular O_2 levels of HeLa was indicated with $[Ru(dpp)_3]^{2+}Cl_2$ {tris (4, 7-diphenyl-1,10-phenanthroline) ruthenium (II) dichloride}. DNFs@ZnMn (200 μg/mL) were incubated with HeLa cells for various time periods, respectively. The O_2 indicator $[Ru(dpp)_3]^{2+}Cl_2$ and Hoechst 33342 were added, with the final concentration of 10 μg/mL and 5 μg/mL, respectively. Then the intracellular fluorescence was recorded by CLSM.

Intracellular ROS generation: DCFH-DA was chosen to detect the intracellular generation of ROS, which can be oxidized to the highly fluorescent DCF by ROS radicals. After incubating HeLa/HUVEC cells in the dark with the samples (200 μg mL^{-1}) for 6 h, noninternalized NCs were washed with PBS. The cells were then irradiated with 660 nm laser (0.2 W cm^{-2}) for 10 min. After irradiation, fresh culture media containing DCFH-DA (20 μM) was added for another 1 h incubation in the dark. And then, the medium was replaced with PBS and fluorescence images of treated cells were acquired using a laser confocal microscope. For DCF detection, the excitation was 485 nm, and the emission wavelength was 525 nm.

Measurement of Intracellular GSH: To evaluate the inhibition effect of DNFs@ZnMn on intracellular GSH, HeLa cells (≈1×10^5) were seeded in 96-well plates and incubated

using the protocol above. When the cells confluence reached 70%, the cells were washed with PBS three times and media containing different samples were added including PBS, DNFs, DNFs-n1@ZnMn, DNFs-n2@ZnMn and DNFs@ZnMn (200 μg mL^{-1}) with/without 660 nm laser irradiation for 24 h. The cells were further cultured for 24 h and measured on enzyme labeled instrument system to measure changes in intracellular GSH levels according to the manufacturer's protocol (Bain-marie Biotech, China).

Mitochondrial membrane potential: HeLa cells seeded in 6-well plates and allowed to grow overnight at 37°C under 5% CO_2. Then, cells were treated with PBS, DNFs, DNFs-n1@ZnMn, DNFs-n2@ZnMn and DNFs@ZnMn (200 μg mL^{-1}) with/without 660 nm laser irradiation for 24h. After that, the cells were irradiated with 660 nm laser (0.2W/cm^2, 10 mins). After staining with JC-1 for 30 mins, the cells were measured by CLSM.

Investigating the mPTP opening: To examine the mPTP, 4T1 cells were seeded in 35-mm glass-bottom cell culture dishes at a density of 2.0×10^5 cells per well and cultured for 24 h. The medium was then replaced with 1.0 mL of fresh medium and treated with PBS, DNFs, DNFs-n1@ZnMn, DNFs-n2@ZnMn and DNFs@ZnMn (200 μg mL^{-1}) with/without 660 nm laser irradiation for 24 h. After washing with PBS, cells or sections were incubated with the corresponding working solution (Calcein-AM loading/ $CoCl_2$) (200 nM) at 37°C for 20 min. Subsequently, the cells were stained by Hoechst 33342 (5 μg/mL) for another 20 min and detected by CLSM.

Quantitative reverse transcription polymerase chain reaction (qRT-PCR) analysis of mRNA expression: HeLa cells were seeded into 6-well culture plates and cultured for 24 h, followed by removing the culture medium and adding PBS, DNFs, DNFs-n1@ZnMn, DNFs-n2@ZnMn and DNFs@ZnMn (200 μg/mL) into 6-well culture plates, respectively. After 6 h, the medium was replaced with fresh medium and the cells were further incubated for 48 h. During the process, cells were washed three times with ice-cold PBS. Total RNA was isolated using a total RNA extraction kit (Solarbio) and then purified total mRNA was reverse transcribed using the Fast King RT kit (With gDNase)

to generate cDNA. The amount of ATG-5 mRNA was analyzed by real-time qRT-PCR. The primer sequences used in the analysis were listed as follows:

ATG-5 forward:

5'- AAGATCACAAGCAACTCTGG/rA/rU/GGGATTGCAAAATGACAG -3';

β-actin forward: 5'-TAGTTGCGTTACACCCTTTCTTG-3';

Western blot assay: The HeLa cells were seeded into 6-well culture plates and cultured for 24 h, followed by removing culture medium and adding corresponding materials. After 6 h, the medium was replaced with fresh medium and further incubated for 48 h. Subsequently, the solutions were removed and the cells were washed thrice with ice-cold PBS and treated with 350 μL SDS lysis buffer. The cell lysates were heated at 100°C for 10 min. The concentrations of protein were measured by the BCA protein assay kit. The proteins were separated on 10% SDS-polyacrylamide gel electrophoresis with SDS loading buffer and then electro-transferred onto a PVDF transfer membrane with WB Transfer Buffer at 220 mA for 2.5 h. The membranes were blocked with 5% nonfat dry milk in TBST buffer for 1 h at room temperature. The membranes were incubated overnight at 4°C with corresponding antibodies in TBST containing 5% nonfat dry milk. After three times of successive washes with TBST for 10 min, the membranes were incubated with secondary antibodies in TBST containing 5% nonfat dry milk for 1 h at room temperature. After three times of successive washes with TBST for 10 min, protein expressions were determined using a Super Signal chemiluminescence system (ECL) and photographed by automatic chemiluminescence image processing system (Tannon-4600SF).

Measurement of Intracellular AO and LPO: To assess the intracellular AO production, HeLa cells were pre-seeded in optical cultured dishes were treated with PBS, DNFs, DNFs-n1@ZnMn, DNFs-n2@ZnMn and DNFs@ZnMn (200 μg mL^{-1}) with/without 660 nm laser irradiation for 24 h. After being washed with PBS for 3 times, those cells were stained with AO (10 μM) for 35 min. The fluorescent emission of AO (λ_{Ex} = 488 or 561 nm) from was detected using CLSM to test intracellular AO.

To assess the intracellular LPO production, HeLa cells pre-seeded in optical cultured

dishes were treated with PBS, DNFs, DNFs-n1@ZnMn, DNFs-n2@ZnMn and DNFs@ZnMn (200 μg mL^{-1}) with/without 660 nm laser irradiation for 24 h. After being washed with PBS for 3 times, those cells were stained with 10 μM of LPO and Hoechst (1 μg/mL) for 35 min, respectively. Finally, the fluorescent emission of LPO (λ_{Ex} = 488 nm, λ_{Em} = 530 nm) from those cells was detected using CLSM to test intracellular LPO.

Measurement of intracellular pH changes: To determine the intracellular pH changes, cells were pre-seeded in cell view 35-mm glass-bottom cell culture dishes with four compartments for 24 h, and then incubated with PBS, DNFs, DNFs-n1@ZnMn, DNFs-n2@ZnMn and DNFs@ZnMn (200 μg mL^{-1}) with/without 660 nm laser irradiation for 24 h. Next, those cells were stained with BCECF-AM (2.5 μM) for 30 min. After washing three times with PBS, the intracellular fluorescent emission of BCECF-AM was observed by Nikon A1 plus confocal laser scanning microscope (λ_{Ex} = 488 nm, λ_{Em} = 500-550 nm). For quantitation of intracellular pH value, the intracellular pH was equilibrated to the surrounding medium through the H^+/K^+ ionophore nigericin (10 μg/mL). Briefly, cells were pre-seeded in 35-mm glass-bottom cell culture dishes for 24 h, and then incubated with H^+/K^+ ionophore nigericin of different pH values (pH = 5.5, 6.0, 6.5, 6.8, 7.0 and 7.4). Next, those cells were stained with BCECF-AM (2.5 μM) for 40 min at 37°C in dark. After being washed three times with PBS, the intracellular fluorescent emission of BCECF-AM was observed by confocal laser scanning microscope (λ_{Ex} = 488 nm, λ_{Em} = 500-550 nm). The relative fluorescent intensity was quantified via ImageJ software.

Ad-mCherry-EGFP-LC3B transfection assay: To evaluate the autophagy flux, HeLa cells seeded in 6-well plates were transfected with LC3 adenovirus conjugated with mCherry-EGFP-LC3B for 48 h at 37℃. After the different treatments, the samples with the red/green fluorescence were visualized using CLSM.

Evaluation of autophagy *in vitro*: HeLa cells (1×10^5 cells/well) were seeded in glass cover slips overnight and treated with above mentioned nano-formulations. Then the cells were incubated with Lysotracker Red first for 30 min and then were fixed by 4% polyformaldehyde. After that, the cells incubated with LC3B primary antibody

overnight and AF488-labeled goat anti-rabbit secondary antibody for 1 h. Subsequently, cells were washed three times by PBS and stained with hoechest (5 μg/mL) for 5 min, imaged by CLSM to observe the colocalization between lysosome and LC3B autophagosomes.

IL-1β assays: HeLa cells were seeded into 96-well plates overnight, and then incubated with PBS, DNFs, DNFs-n1@ZnMn, DNFs-n2@ZnMn and DNFs@ZnMn (200 μg mL^{-1}) with/without 660 nm laser irradiation for 24 h, respectively. The release of IL-1β was detected by the IL-1β assay kit according to the manufacturer's protocols.

Lactate dehydrogenase (LDH) assays: HeLa cells were seeded into 96-well plates overnight, and then incubated with PBS, DNFs, DNFs-n1@ZnMn, DNFs-n2@ZnMn and DNFs@ZnMn (200 μg mL^{-1}) with/without 660 nm laser irradiation for 24 h, respectively. The release of LDH was detected by the LDH cytotoxicity assay kit according to the manufacturer's protocols.

Adenosine triphosphate (ATP) release detections: HeLa cells were seeded into 96-well plates overnight, and then incubated with PBS, DNFs, DNFs-n1@ZnMn, DNFs-n2@ZnMn, DNFs@ZnMn (200 μg mL^{-1}) with/without 660 nm laser irradiation for 24 h, respectively. The release of ATP was detected by the ATP assay kit according to the manufacturer's protocols.

Cell morphology observation: HeLa cells were cultured on sterilised cover slips in 24-well plates overnight, and then incubated with PBS, DNFs, DNFs-n1@ZnMn, DNFs-n2@ZnMn and DNFs@ZnMn (200 μg mL^{-1}) with/without 660 nm laser irradiation for 24 h, respectively. The morphology of cells was further observed by Confocal laser scanning microscopy (CLSM).

Cytotoxicity assay: Cell cytotoxicity was measured by the MTT method under normoxia (21% oxygen) or hypoxia (2% oxygen). HeLa cells were seeded in 96-well plates (2.5×10^3 cells per well) overnight. Subsequently, the cells were incubated with PBS, DNFs, DNFs-n1@ZnMn, DNFs-n2@ZnMn and DNFs@ZnMn for 24 h under normoxic and hypoxic conditions, respectively. After that, the cells were exposed to a 660 nm laser (0.2 W cm^{-2}, 10 min) for photodynamic therapy groups, and then all

groups were further incubated for 24 h. In addition, HeLa cells were seeded in 96-well plates (2.5×10^3 cells per well) overnight. Subsequently, the cells were incubated with PBS, DNFs, DNFs-n1@ZnMn, DNFs-n2@ZnMn and DNFs@ZnMn for 24 h. Before testing, the cells were treated with 10 μL MTT reagents at 37 °C for 2 h in dark via the protocol. The optical density (OD) at 450 nm was obtained by using the microplate reader. The cell viability was calculated as follows:

Cell viability (%) = $(OD_{Samples}/OD_{PBS}) \times 100\%$

Where $OD_{Samples}$ and are OD_{PBS} represent the OD value at 450 nm after different materials and PBS treatments.

Dead/live staining: HeLa/HUVEC cells were seeded on Chambered cover glass at 37°C for 24 h. After which, previous medium was replaced by fresh medium that contained PBS, DNFs, DNFs-n1@ZnMn, DNFs-n2@ZnMn and DNFs@ZnMn (200 μg/mL) with/without 660 nm laser irradiation, respectively. After co-culture for 24 h, cells were stained with calcein AM (5 μL) and PI (10 μL) for 20 min and then observed using confocal microscop.

HeLa Cells were seeded in 6-well plates with a density of 2×10^5 cells per well for 8 h and then treated with free PBS, DNFs, DNFs-n1@ZnMn, DNFs-n2@ZnMn and DNFs@ZnMn (200 μg/mL) with/without 660 nm laser irradiation for 24 h, respectively. The supernatant and the cell monolayer were collected, washed twice with cold PBS. Then, they were stained with Alexa Fluor 488 annexin V and Propidium Iodide using an Alexa Fluor 488 annexin V/Dead cell apoptosis kit according to the manufacturer's instructions. After staining, the percentage of apoptotic cells was examined with flow cytometry.

Xenograft tumor model in mice: All animal experiment protocols were reviewed and approved by the Animal Care and Use Committee of Institute of Beijing Normal University and complied with all relevant ethical regulations. The female BALB/c nude mice (18-20 g, 5 weeks) were purchased from Beijing Charles River Laboratory Animal Center and raised in a specific pathogen-free grade laboratory. The HeLa tumor-bearing mice model was established by subcutaneously inoculating about 5×10^6 cells

in the right flank of BALB/c nude mice.

***In vivo* Imaging:** When the average tumor volume reached 100-120 mm^3, the mice were intravenously injected with PBS, DNFs, DNFs-n1@ZnMn, DNFs-n2@ZnMn and DNFs@ZnMn at 3 mg/kg dosages, respectively. Fluorescence imaging data were collected using the IVIS Lumina II *in vivo* imaging system at 6 h post-injection. The mice were euthanized and the main organs (liver, kidney, spleen, lung, and heart) of the mice were selected for ex *vivo* imaging by IVIS Lumina II in the *vivo* imaging system.

Tumor growth inhibition: For *in vivo* antitumor study, the mice were randomly divided into 5 groups (four mice per group) for the treatment to obtain the tumor volume of about 100-120 mm^3. 200 μL of therapeutic nanoagents was injected into each nude mouse via tail vein every other day for 14 days and meanwhile tumor weight and size were monitored. Tumor size was measured by a caliper and the tumor volume was calculated according to the following formula:

tumor volume (mm^3) = length×$width^2$/2

After 14^{th} therapy, tumors and major organs were sectioned for hematoxylin-eosin staining (H&E) analyses.

Hemolysis test: Red blood cells (RBCs) were collected and purified to be resuspended in 5 mL saline. 0.2 mL of RBCs was incubated with 0.8 mL DNFs@ZnMn in saline with different concentrations for 30 min at 37℃, respectively. DNFs@ZnMn, saline (negative control) and MQ (positive control) were incubated with RBCs, respectively. After centrifugation (6010 g, 5 min), the supernatant was obtained to detect the absorbance at 570 nm with a microplate reader. The hemolysis (%) was calculated by the following equation:

$$Hemolysis = \frac{Asample - Anegative}{Apositive - Anegative} \times 100\%$$

where A sample is the absorbance of supernatant after incubation of blood and materials, $A_{negative}$ and $A_{positive}$ are the absorbance of supernatant after incubation of saline and H_2O, respectively.

***In vivo* biodistribution:** The tumor model was established via subcutaneous

inoculation of HeLa cells (50 μL of 2 × 10^7 cells/mL) into the right armpit of female BALB/c mice (20 ± 2 g). When the tumor volume reached 50-100 mm^3, the mice were randomly divided into three groups. Different formulations including PBS, DNFs, DNFs-n1@ZnMn, DNFs-n2@ZnMn, DNFs@ZnMn (3 mg/kg) all labeled with Cy5, which were intravenously injected. *In vivo* imaging was performed with a Berthold NightOWL LB 983 NC100 imaging system (Berthold,Germany) with excitation and emission wavelengths of 630 and 700 nm, respectively. The kinetic fluorescence distributions of Cy5 at 0 h, 3 h, and 6 h post-dosing was imaged and recorded. To further verify the biodistribution of the PBS, DNFs, DNFs-n1@ZnMn, DNFs-n2@ZnMn and DNFs@ZnMn, the mice were euthanized after 24 h and the tumors and major organs were collected.

Serum biochemistry test: Blood samples (1 mL, n = 3) were collected from the eyeball after different treatments. The serum was obtained through centrifugation at 845 rcf for 10 min. Serum levels of albumin (ALB), alanine transferase (ALT), alkaline phosphatase (ALP), total protein (TP), total bilirubin (TBIL), globulin (GLO), creatinine (CREA), urea (UREA), aspartate aminotransferase (AST), lactate dehydrogenase (LDH), creatine kinase (CK) and creatine kinase MB (CK-MB) were measured using the commercial kits.

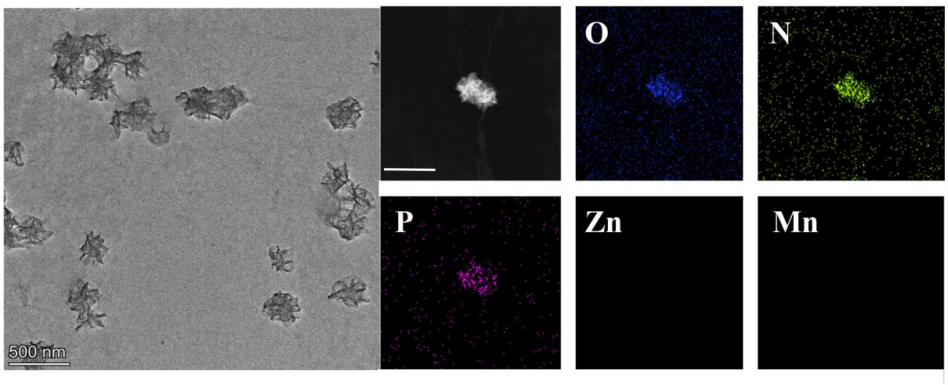

Fig. S1 TEM images and corresponding element mapping analysis of DNFs.

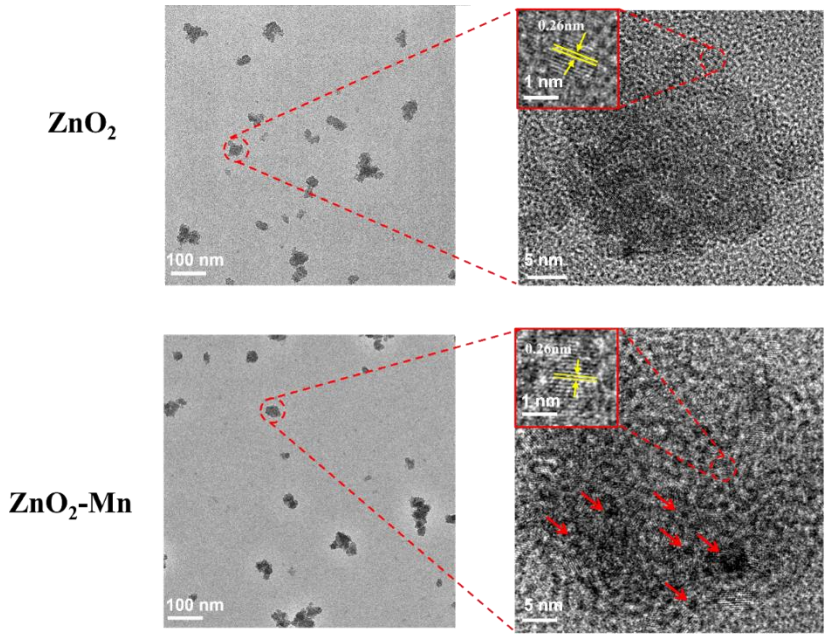

Fig. S2 TEM image and corresponding element mapping analysis of ZnO_2 and ZnO_2-Mn.

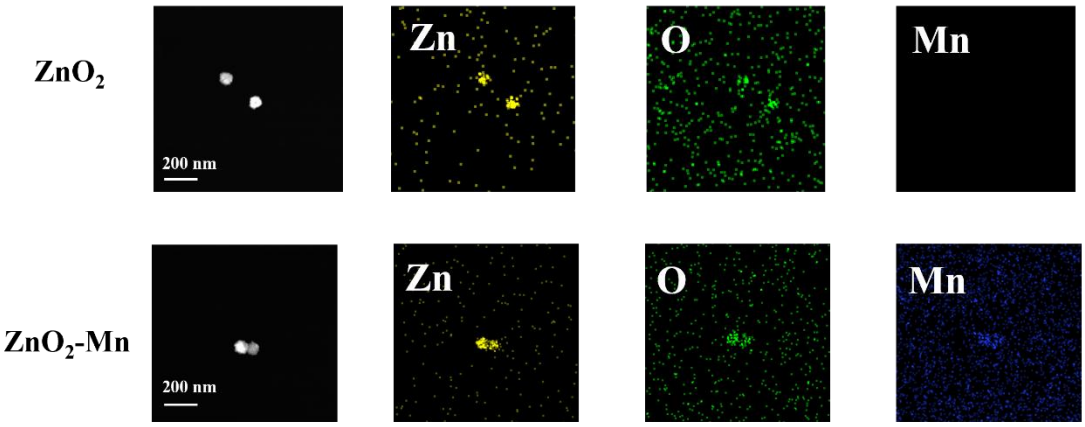

Fig. S3 HAADF-STEM image and corresponding element mapping analysis of ZnO_2 and ZnO_2-Mn.

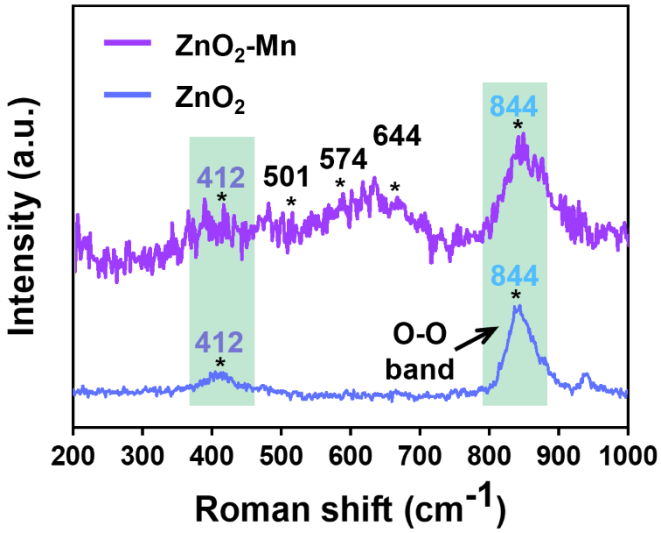

Fig. S4 Roman spectra of ZnO_2 and ZnO_2-Mn.

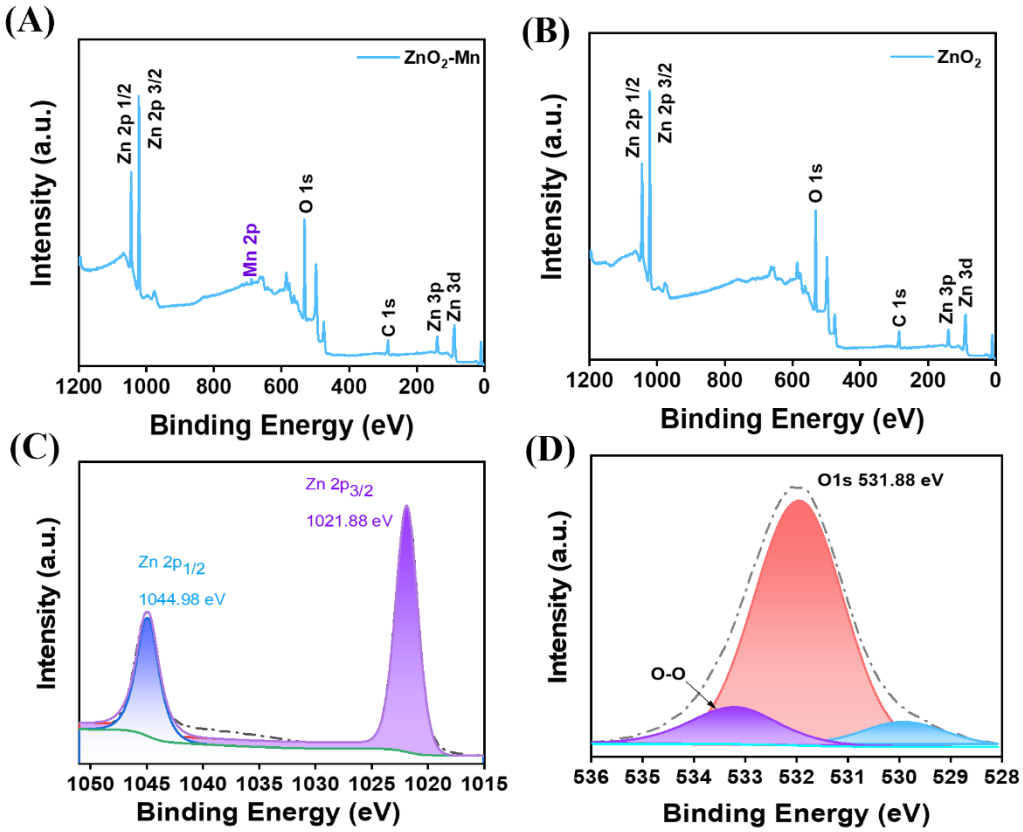

Fig. S5 XPS analysis to confirm the elemental composition of ZnO_2-Mn.

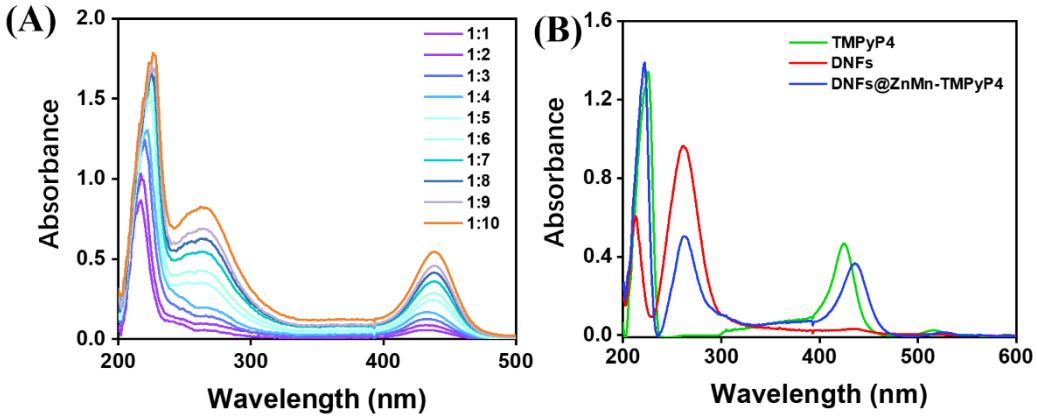

Fig. S6 Evaluation on the loading of TMPyP4 in DNFs@ZnMn based on UV-vis absorption of TMPyP4. (A) Absorbance of TMPyP4-DNA prepared with different ratios of TMPyP4 to AS1411 aptamer. (B) Absorbance of TMPyP4, DNFs, and DNFs@ZnMn-TMPyP4 at a loading ratio of 1:10.

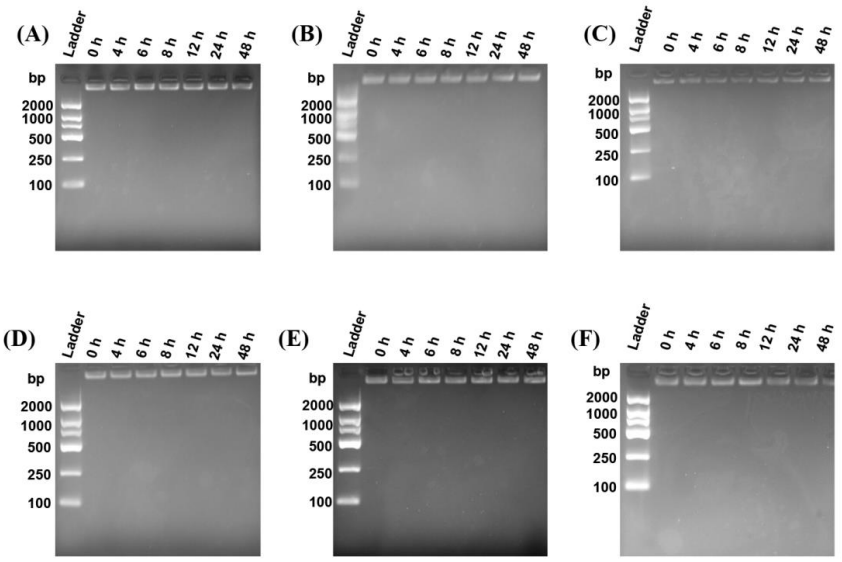

Fig. S7 Evaluation of the stability of nanocarriers by agarose gel electrophoresis analysis. DNFs (A) and DNFs@ZnMn (B) after a preassigned incubation in a DMEM medium with 10% fetal bovine serum. DNFs (C) and DNFs@ZnMn (D) in PBS. DNFs (E) and DNFs@ZnMn (F) in water.

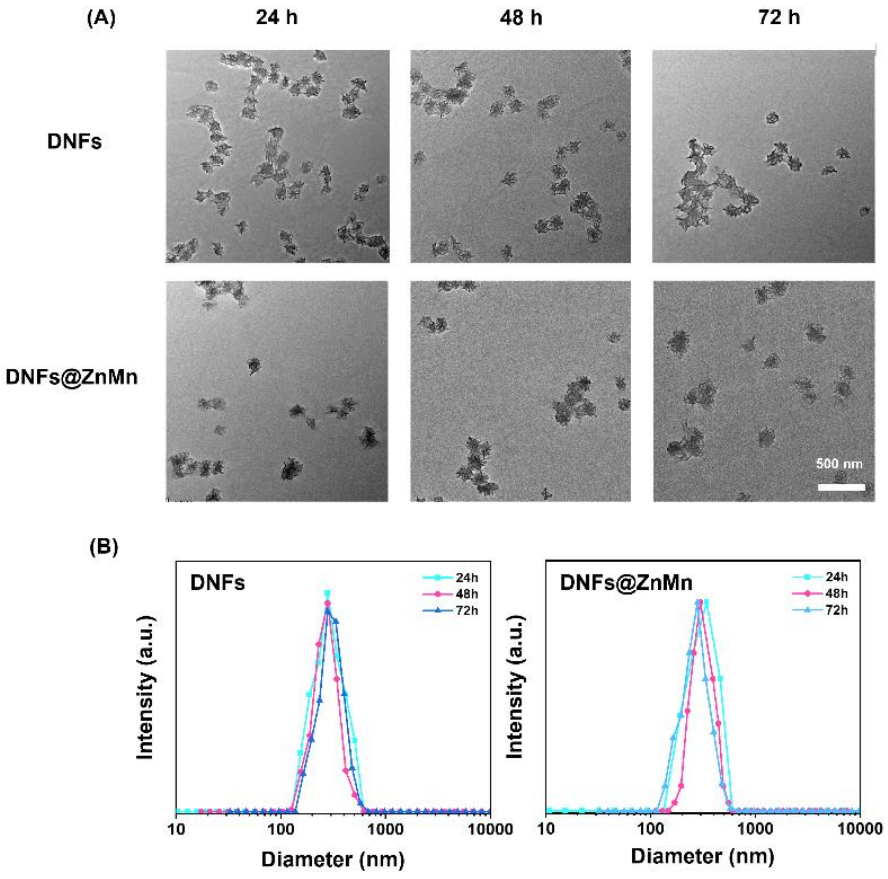

Fig. S8 Evaluation on the long-term stability of DNFs and DNFs@ZnMn. (A) TEM images of two species at different times. (B) Dynamic light scattering analysis in PBS buffer (pH=7.4).

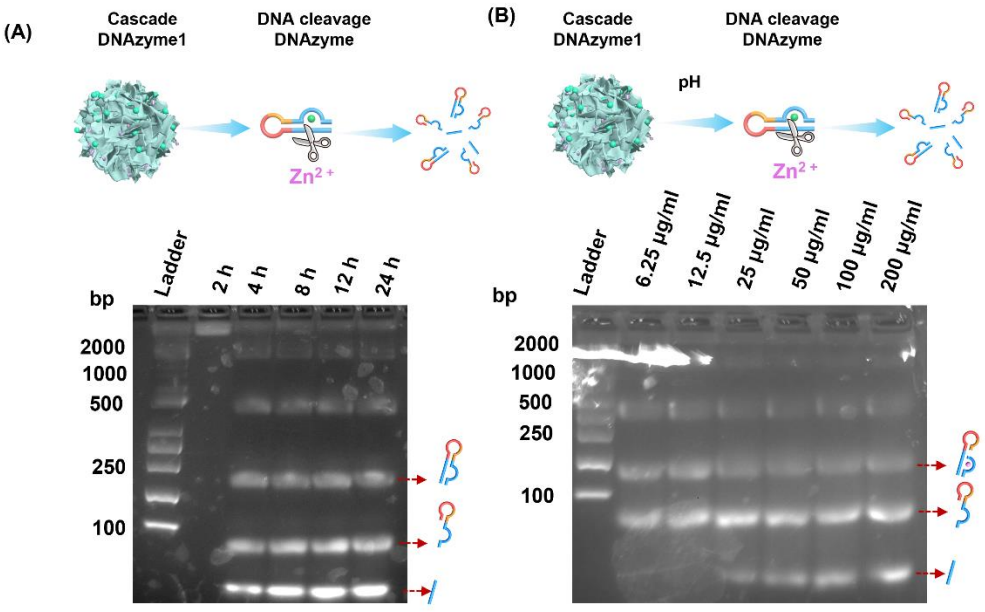

Fig. S9 Evaluation of catalytic DNA cleavage efficiency of the DNAzyme by PAGE analysis. (A) Adding the same concentration of Zn^{2+} into the reaction system and incubating for different times. (B) Treating DNFs@ZnMn with PBS (pH~6.5) to release metal ions for promoting the cleavage of DNA substrate.

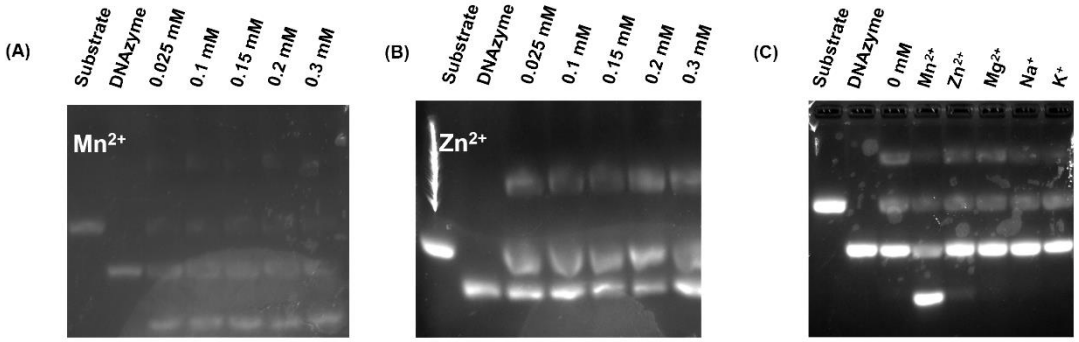

Fig. S10 Catalytic cleavage efficiency of the substrate at different concentrations of metal ions. (A) Mn^{2+}. (B) Zn^{2+}. (C) Different metal ions at the same concentration of 0.2 mM.

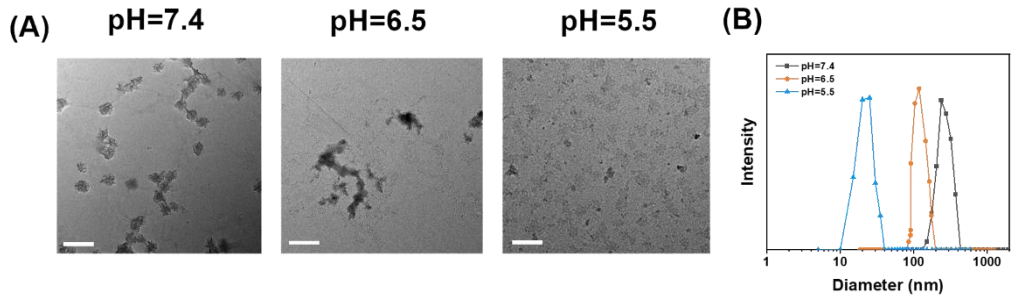

Fig. S11 TEM image (A) and DLS (B) of DNFs@ZnMn at different pH values. Scale bars: 500 μm

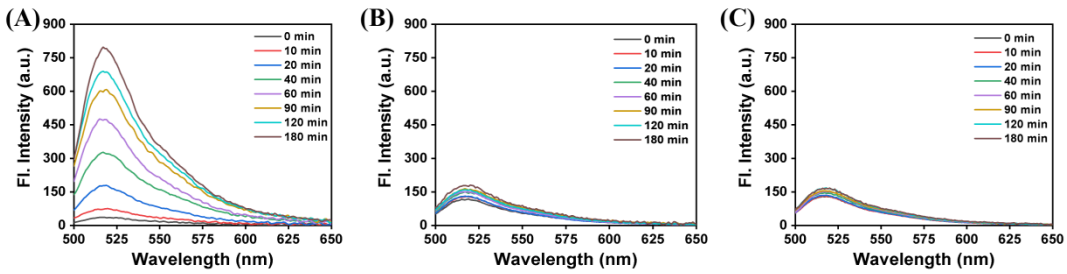

Fig. S12 (A) FL spectra emitted from the cleavage of DNFs@ZnMn at different times. (B) Fluorescence spectra collected upon DNAzyme-mediated DNFs-n1@ZnMn cleavage. (C) Fluorescence spectra collected upon DNAzyme-mediated DNFs-n2@ZnMn cleavage.

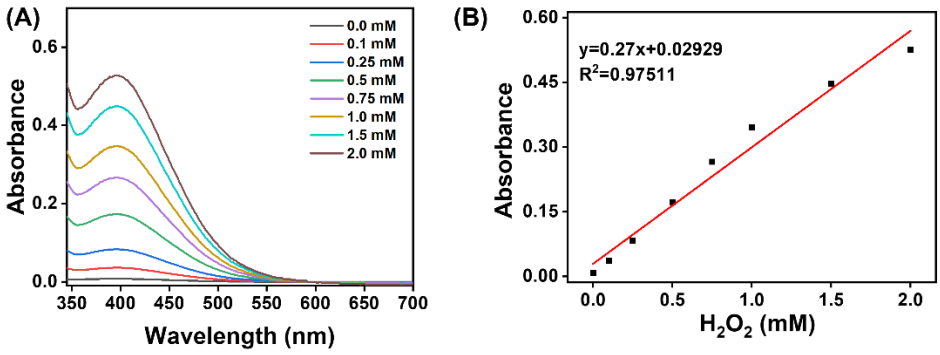

Fig. S13 The standardization for evaluating H_2O_2 by $Ti(SO_4)_2$. (A) The UV−vis absorption of $Ti(SO_4)_2$ (1 mg/mL) treated with different concentration of H_2O_2 with DNFs@ZnMn (1 mg/mL) added in PBS buffer (pH 6.5). (B) The linear relationship between $Ti(SO_4)_2$ absorption at 412 nm and H_2O_2 concentration.

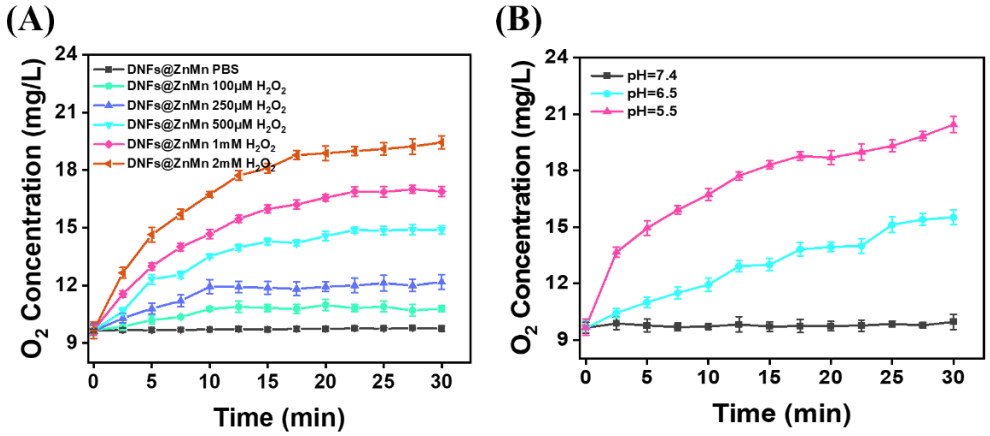

Fig. S14 (A) Time-dependent O_2 generation upon the incubation with different concentration of H_2O_2 with DNFs@ZnMn added in PBS buffer at pH 6.5. (B) Time-dependent O_2 generation upon the incubation at different pH conditions (7.4, 6.5, 5.5) in PBS buffer.

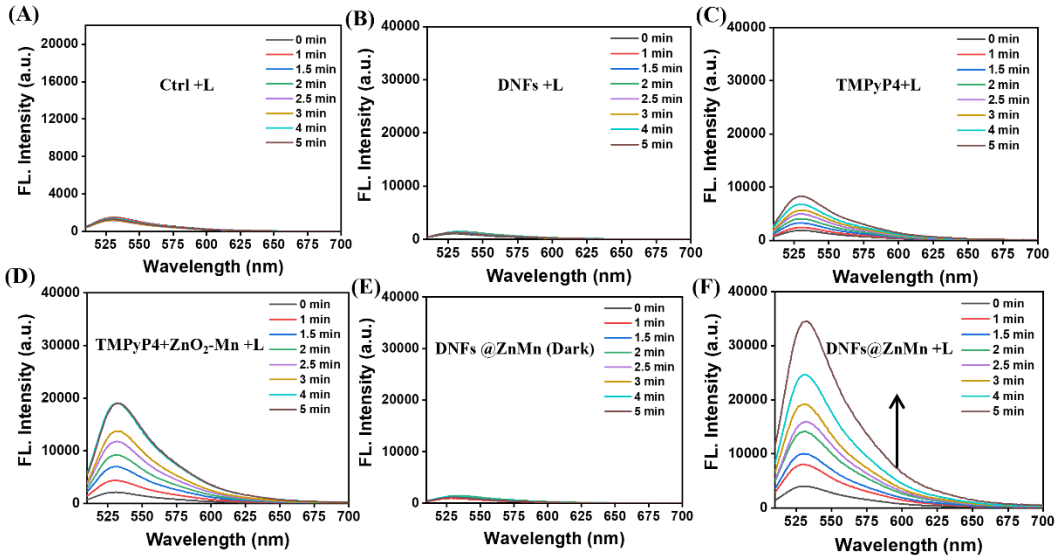

Fig. S15 SOSG fluorescence intensity of different solutions under NIR laser irradiation (0.2 W cm^{-2}).

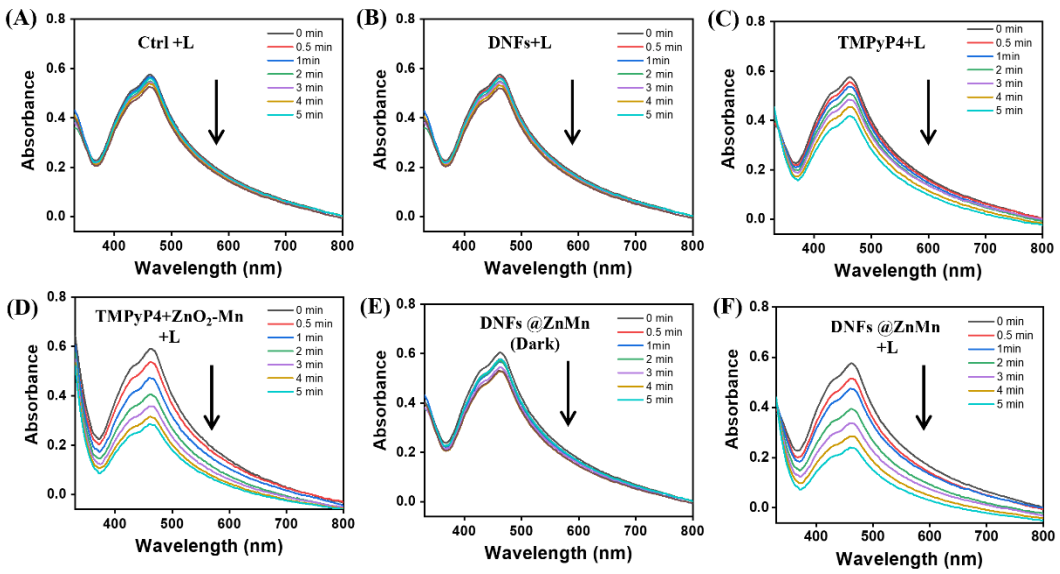

Fig. S16 The decay curves of UV−vis absorption of DPBF at different conditions. (A) Control + Light. (B) DNFs + Light. (C) TMPyP4 + Light. (D) TMPyP4 + ZnO_2-Mn Light. (E) DNFs@ZnMn + Dark. (F) DNFs@ZnMn + Light at various irradiation times. Light irradiation: 660 nm, 0.2 W/cm^2, 10 min.

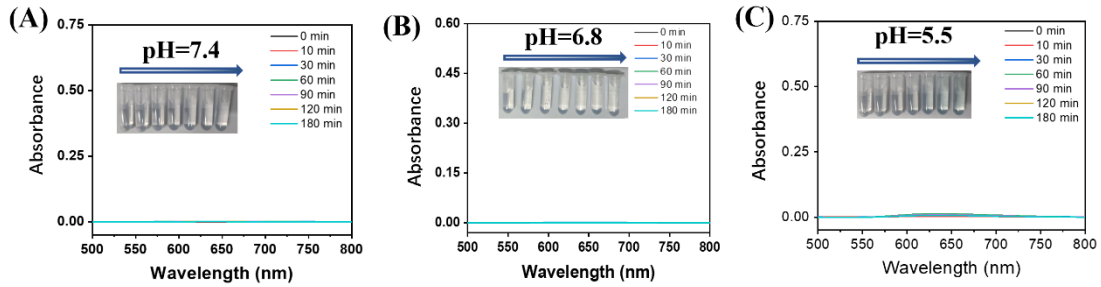

Fig. S17 The UV-vis absorption for ·OH detection by DNFs@ZnMn NPs with TMB as the probe. (A) pH 7.4. (B) pH 6.5. (C) pH 5.5.

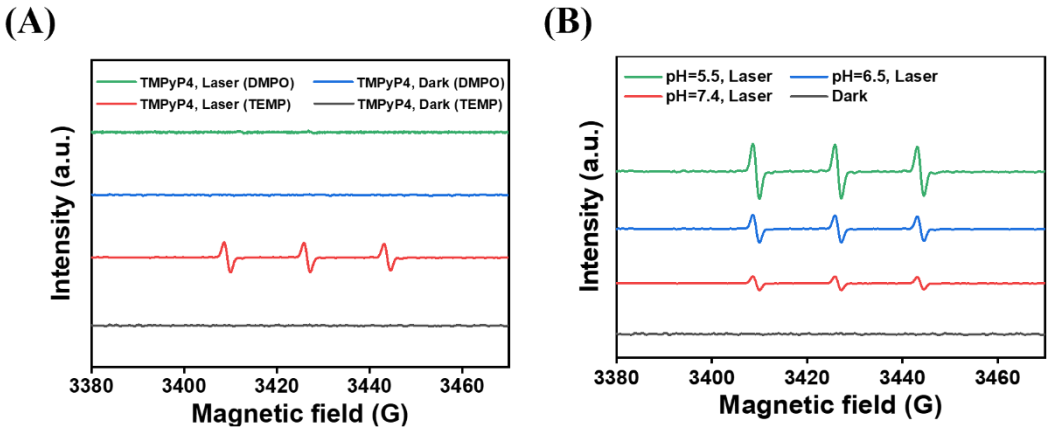

Fig. S18 (A) ESR analysis of ROS species generated from TMPyP4. (B) ESR analysis of DNFs@ZnMn generation $^1O_2$ by TEMP at different pH conditions.

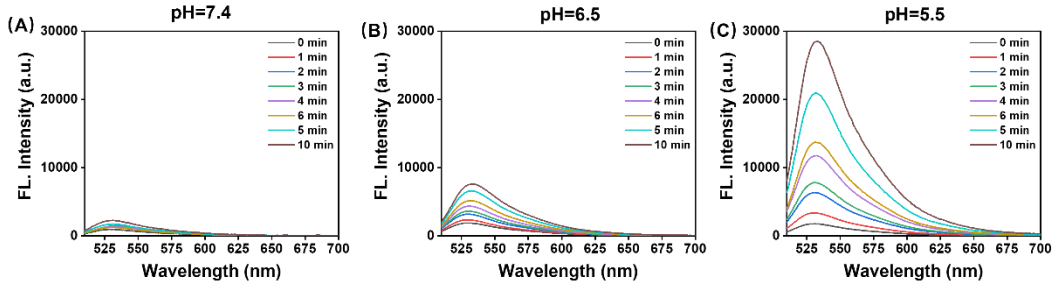

Fig. S19 Evaluation on the generation of $^1O_2$ by DNFs@ZnMn at different pH conditions. (A) pH 7.4. (B) pH 6.5. (C) pH 5.5. The SOSG was selected as the FL probe, based on the FL emission at ~530 nm (under light-irradiation at 660 nm, 0.2 W cm^{-2}).

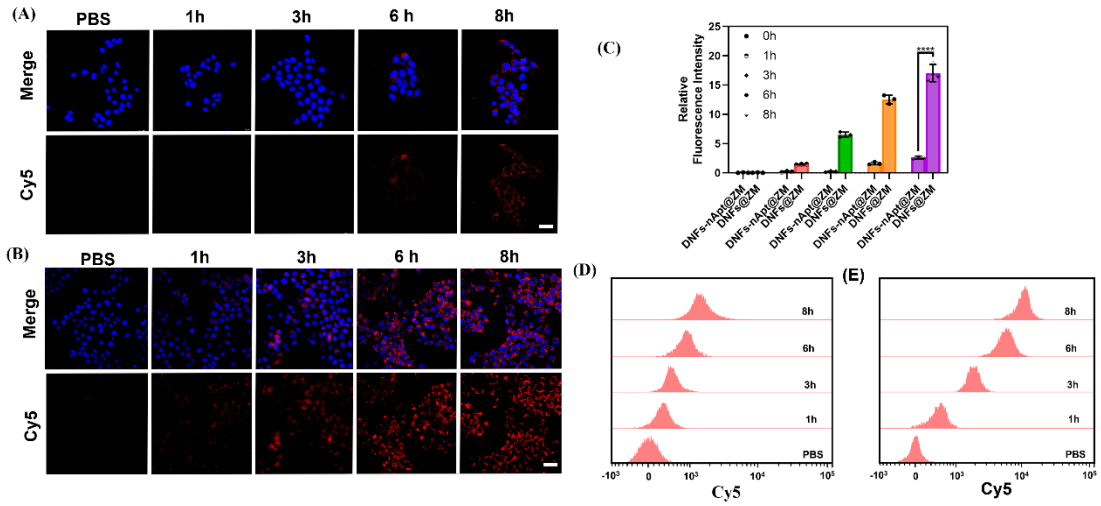

Fig. S20 Confocal microscopic images after incubating DNFs-nApt@ZnMn (A) and DNFs@ZnMn (B) with 4T1 cells for different times. (C) The fluorescence intensity of

each group in (A)/(B). The statistical analysis was performed in contrast to a control group (* p<0.05, ** p<0.01, *** p<0.001, t-test). (D) Flow cytometry after incubating DNFs-nApt@ZnMn with HeLa cells for different times. (E) Flow cytometry after incubating DNFs@ZnMn with HeLa cells for different times. Scale bars: 50 μm.

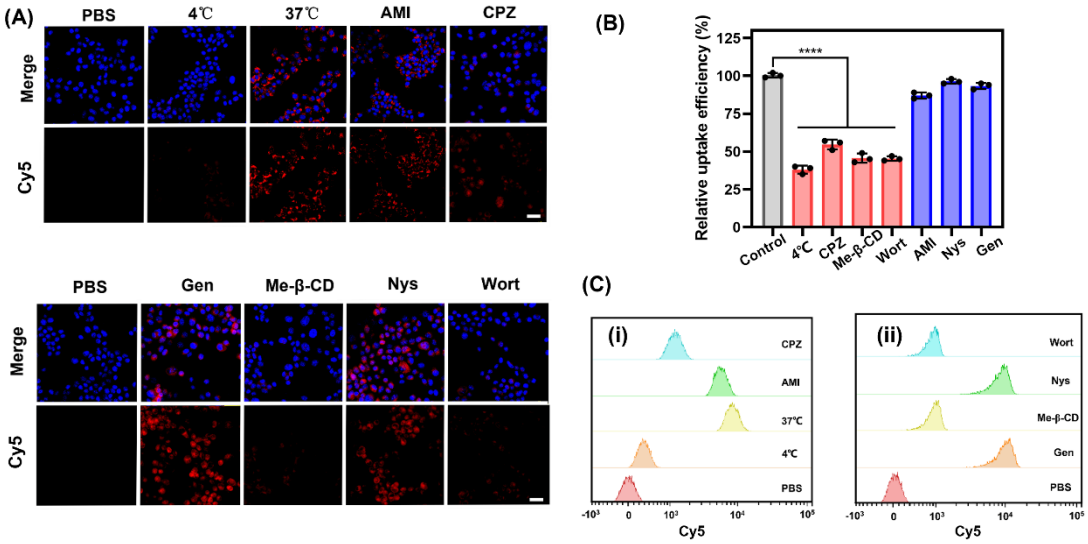

Fig. S21 Study of the endocytosis pathway for DNFs@ZnMn. Confocal images of HeLa cells treated with different endocytosis inhibitors and then incubated with 200 μg/mL DNFs@ZnMn for 4 h. Endocytosis inhibitors including Amiloride (AMI, macro-pinocytosis mediated endocytosis inhibitor), Chlorpromazine hydrochloride (CPZ, clathrin-mediated endocytosis inhibitor), Genistein (Gen, pit mediated endocytosis inhibitor), Methyl-β- cyclodextrin (Me-β-CD, lipid-raft mediated endocytosisinhibitor), Nystatin (Nys, caveolin-mediated endocytosis inhibitor), and wortmannin (Wort, micropinocytosis inhibitor) were employed in the experiment. (B) The fluorescence intensity of each group in (A). The statistical analysis was performed in contrast to a control group (* p<0.05, ** p<0.01, *** p<0.001, t-test). (C) Flow cytometry after incubating DNFs @ZnMn with HeLa cells for different endocytosis inhibitors. Scale bars: 100 μm.

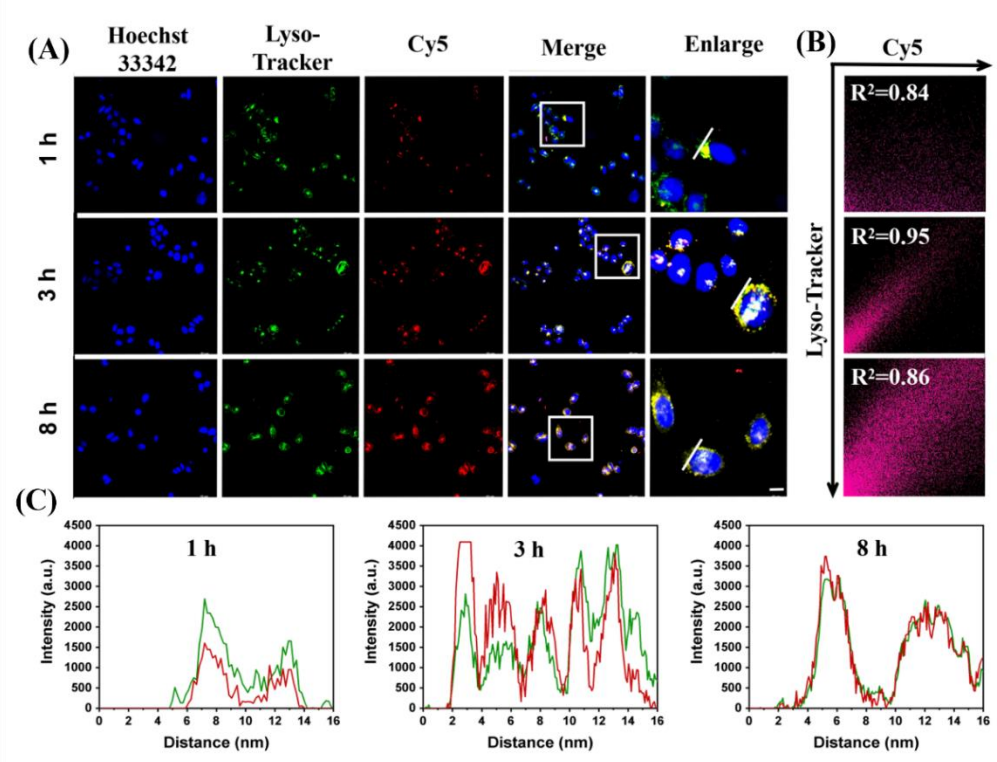

Fig. S22 (A) Colocalization coefficient between the Lysotracker Green and DNFs with different incubation times. (B) PCCs of Lyso-tracker/Cy5. (C) The intensity distribution of Lysotracker Green and DNFs along the arrow in (A). Scale bars: 10 μm.

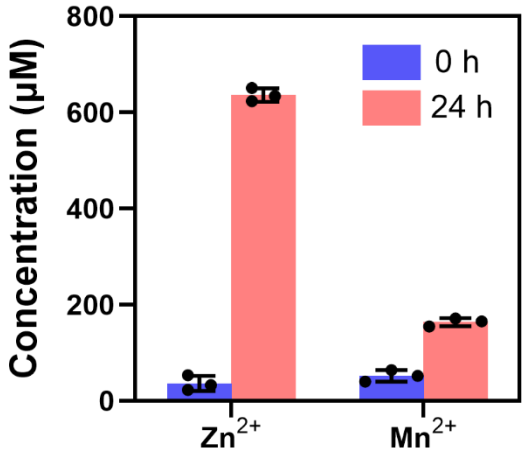

Fig. S23 Profiles of the releasing of Zn^{2+} and Mn^{2+} during the incubation of DNFs@ZnMn in HeLa cells.

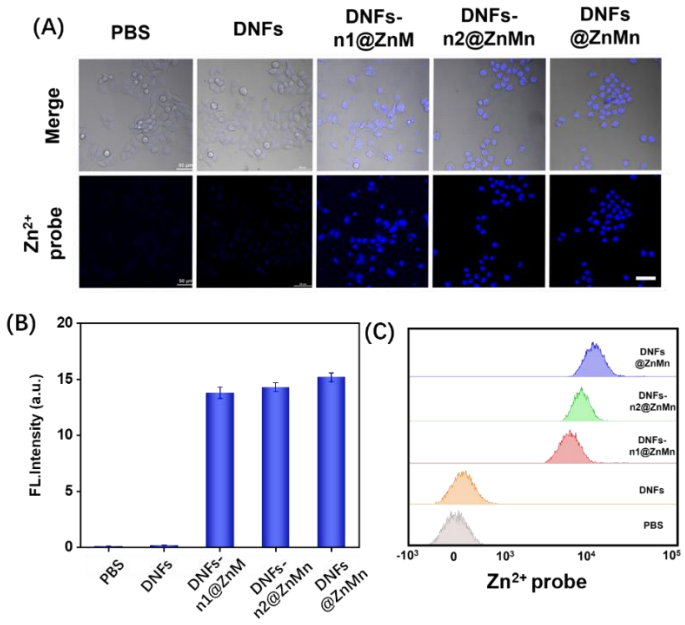

Fig. S24 (A) Fluorescence images of HeLa cells stained with Zn^{2+} dye after incubating with PBS, DNFs, DNFs-n1@ZnMn, DNFs-n2@ZnMn, DNFs@ZnMn. (B) The fluorescence intensity of each group in (A). The statistical analysis was performed in contrast to a control group. (C) Flow cytometry of Zn^{2+} dye fluorescence after incubating PBS, DNFs, DNFs-n1@ZnMn, DNFs-n2@ZnMn, DNFs@ZnMn with HeLa cells. Scale bars: 50 μm.

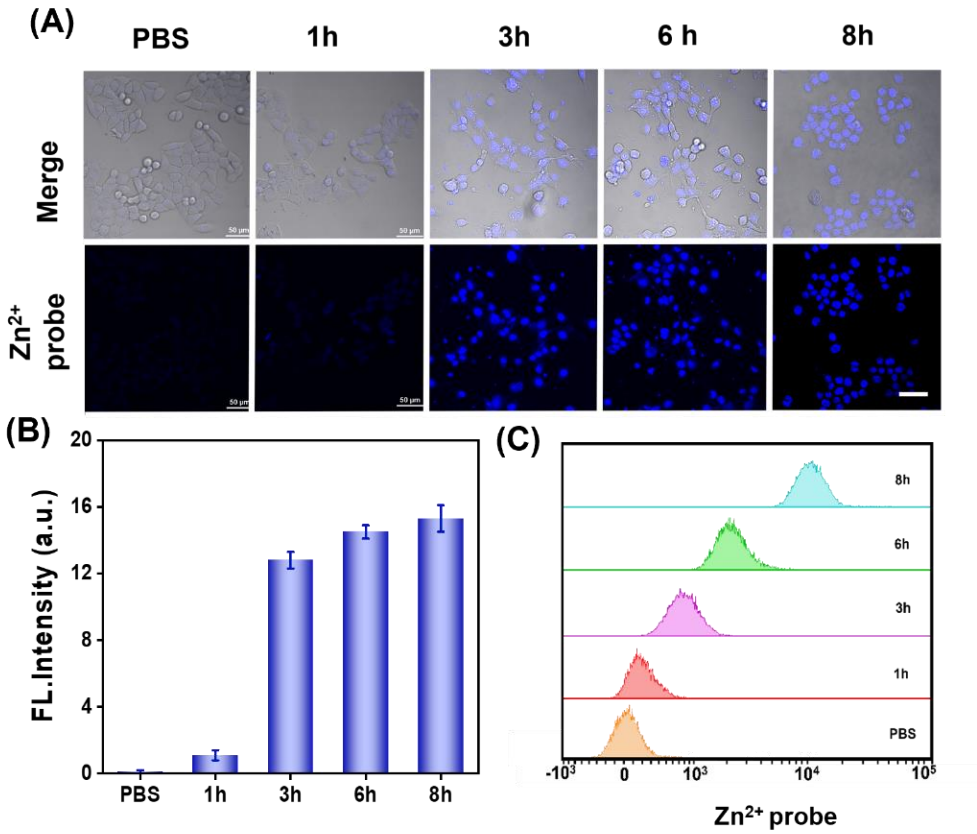

Fig. S25 (A) Fluorescence images of HeLa cells stained with Zn^{2+} dye after incubating with DNFs@ZnMn for different times. (B) The fluorescence intensity of each group in (A). The statistical analysis was performed in contrast to a control group. (C) Flow cytometry of Zn^{2+} dye fluorescence after incubating DNFs @ZnMn with HeLa cells for different time. Scale bars: 50 μm.

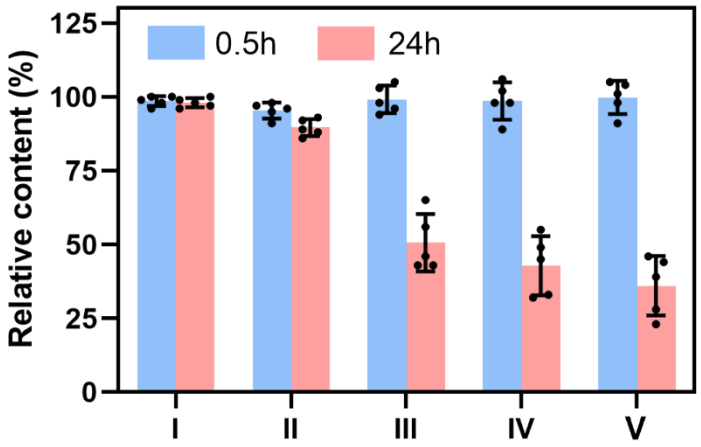

Fig. S26 Evaluation of intracellular H_2O_2 levels by the hydrogen peroxide assay kit. The cells were treated with PBS (I), DNFs (II), DNFs-n1@ZnMn (III), DNFs-n2@ZnMn (IV)

and DNFs@ZnMn (V) for 0.5 h and 24 h, respectively.

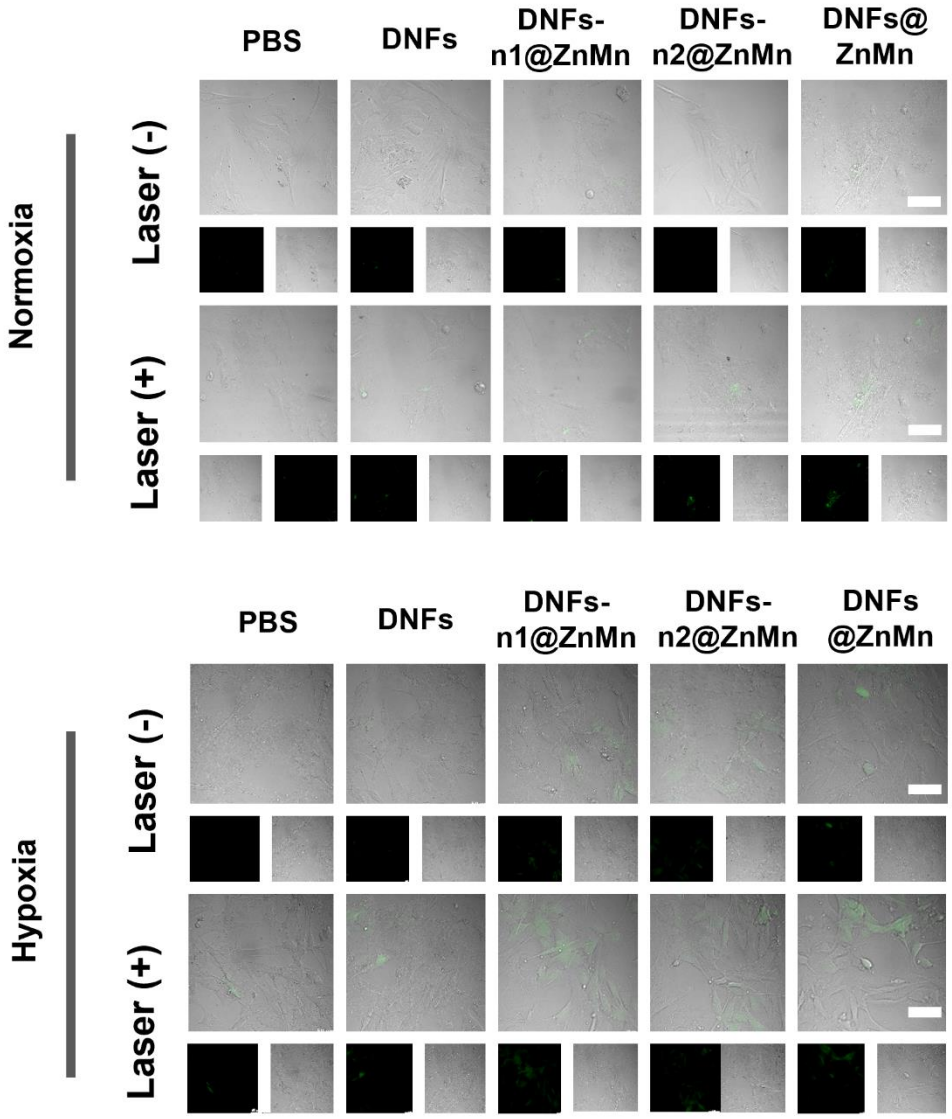

Fig. S27 CLSM images of HUVEC cells stained by SOSG (5 μM) for detecting intracellular $^1O_2$ with PBS, DNFs, DNFs-n1@ZnMn, DNFs-n2@ZnMn and DNFs@ZnMn with/without 660 nm laser irradiation. green channel for SOSG (λ_{Ex} = 488 nm, λ_{Em} = 500−550 nm). Scale bars: 100 μm.

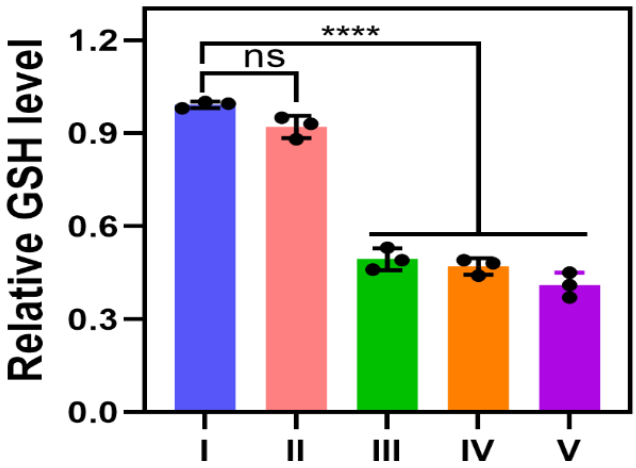

Fig. S28 GSH content of HeLa cells after treating with PBS, DNFs, DNFs-n1@ZnMn, DNFs-n2@ZnMn and DNFs@ZnMn nanomaterials. The statistical analysis was performed in contrast to a control group (* $p<0.05$, ** $p<0.01$, *** $p<0.001$, t-test).

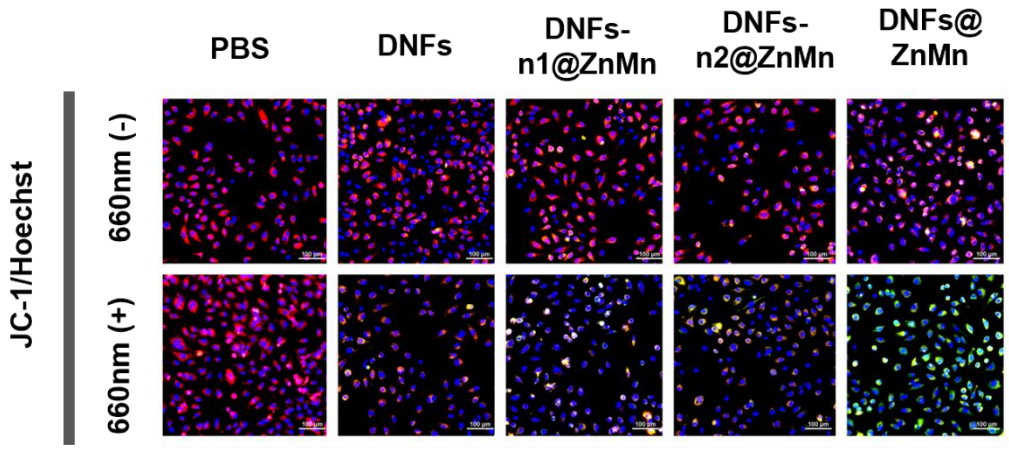

Fig. S29 Evaluation of mitochondrial membrane potential of HeLa cells after treated with PBS, DNFs, DNFs-n1@ZnMn, DNFs-n2@ZnMn and DNFs@ZnMn under Laser (-) / Laser (+) (0.2 W/cm^2 10 min). The probe was JC-1.

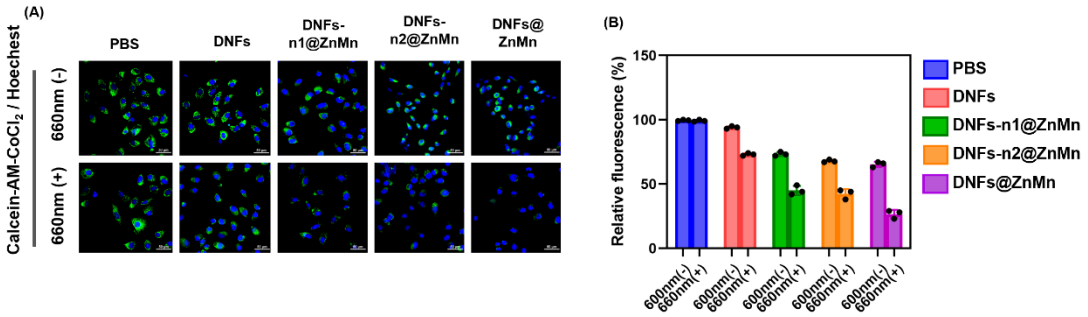

Fig. S30 The evaluation of mitochondrial permeability transition pore (mPTP) during mitochondrial depolarization of HeLa cells by different materials under Laser (-)/Laser (+). (A) FL imaging of HeLa cells by the calcein-AM loading/$CoCl_2$ quenching strategy. (B) Fluorescence intensity of each group.

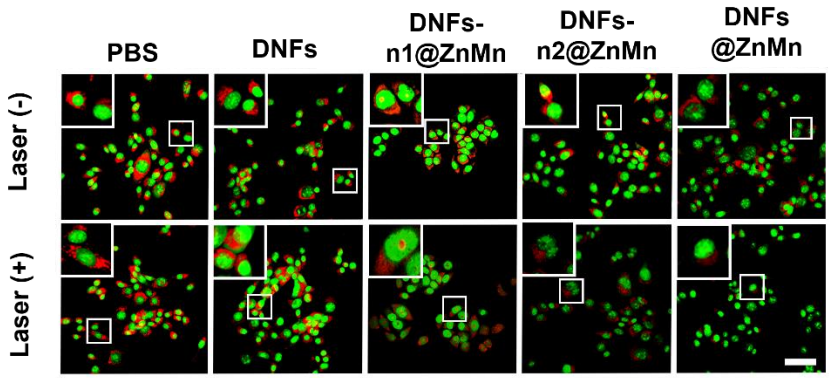

Fig. S31 The imaging of endosomal membrane content after 24 h of the different materials treatment under Laser (-) / Laser (+), based on red signals from AO staining. Scale bars: 50 μm.

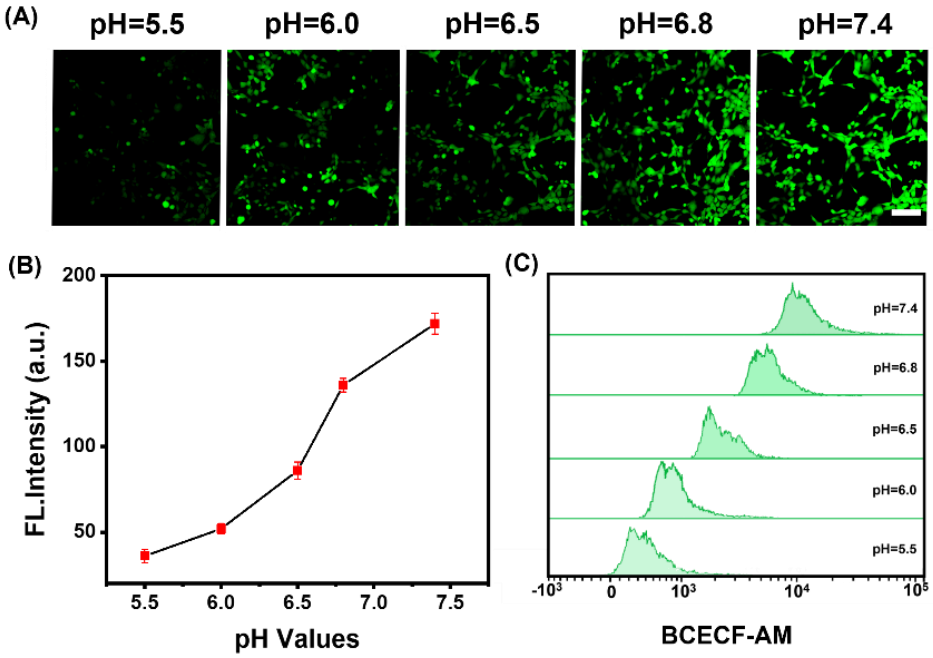

Fig. S32 The reference pH values based on CLSM images of HeLa cells. (A) The pH values (pH = 5.5, 6.0, 6.5, 6.8 and 7.4) were indicated by BCECF-AM (2.5 μM) staining. (B) The quantitative linear relationship of FL responses versus pH values. (C) Flow cytometry analysis of different intracellular pH values (pH = 5.5, 6.0, 6.5, 6.8 and 7.4). Scale bars: 100 μm.

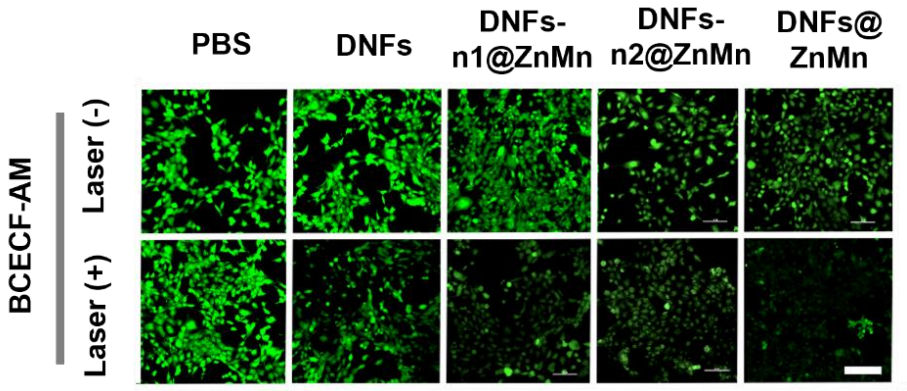

Fig. S33 CLSM images of HeLa cells after treating with PBS, DNFs, DNFs-n1@ZnMn, DNFs-n2@ZnMn and DNFs@ZnMn nanomaterials under Laser (-) / Laser (+). For imaging, the cells were stained by BCECF-AM. Scale bars: 100 μm.

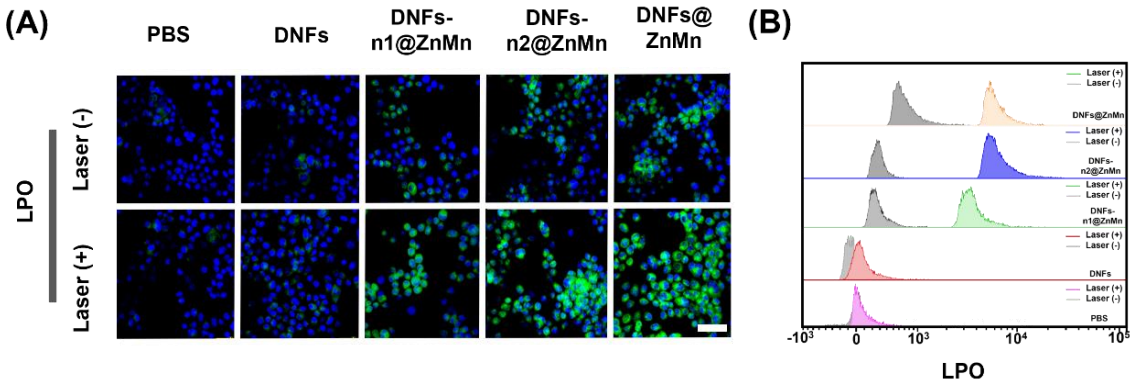

Fig. S34 (A) The imaging of intracellular LPO levels in HeLa cells. (B) Flow cytometric analysis on the intracellular LPO levels in HeLa cell incubated with PBS, DNFs, DNFs-n1@ZnMn, DNFs-n2@ZnMn and DNFs@ZnMn under Laser (-) / Laser (+) for 24 h. Scale bars: 50 μm.

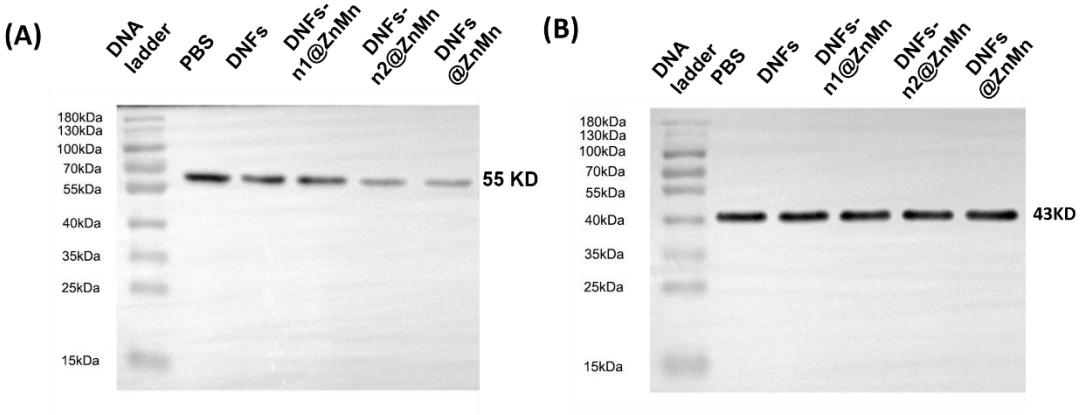

Fig. S35 Western blotting assay to indicate the therapy performance. (A) The intracellular ATG-5 proteins. (B) Control: β-Actin.

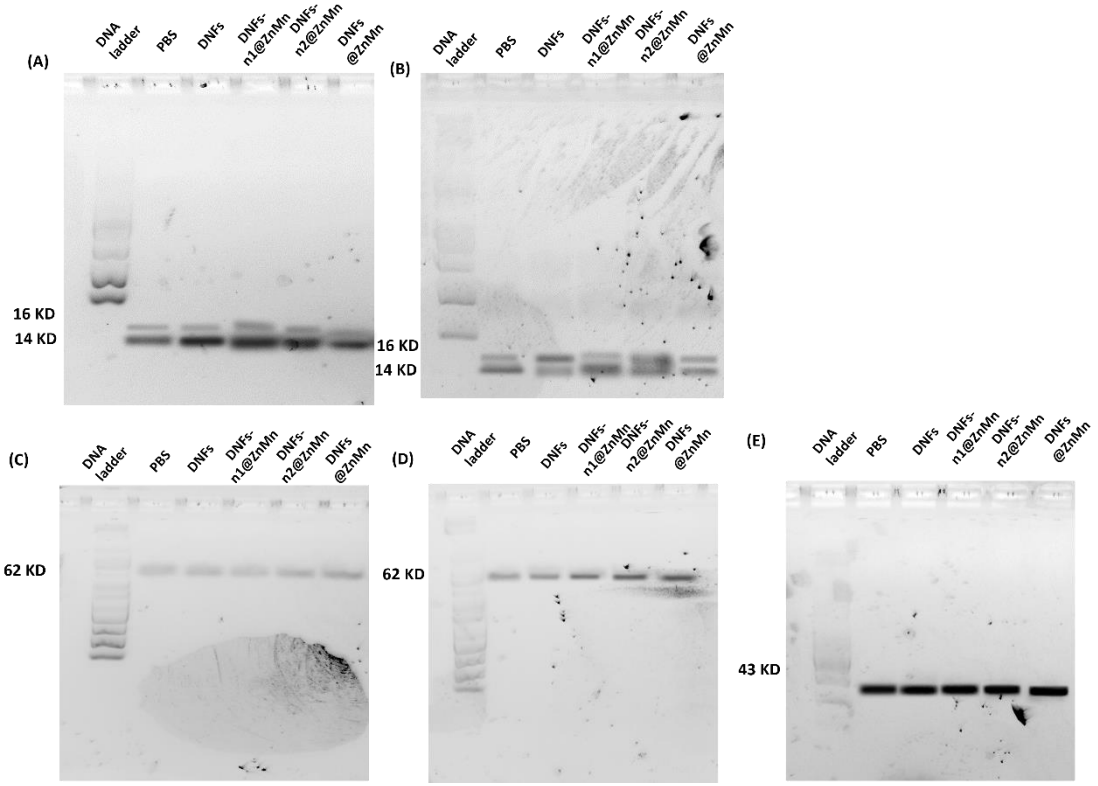

Fig. S36 Western blotting assay to indicate the therapy performance. (A) The intracellular LC3 proteins (660 nm (+)). (B) The intracellular LC3 proteins (660nm (-)). (C) The intracellular p62 proteins (660 nm (-)). (D) The intracellular p62 proteins (660nm (+)). (E) Control: β-Actin.

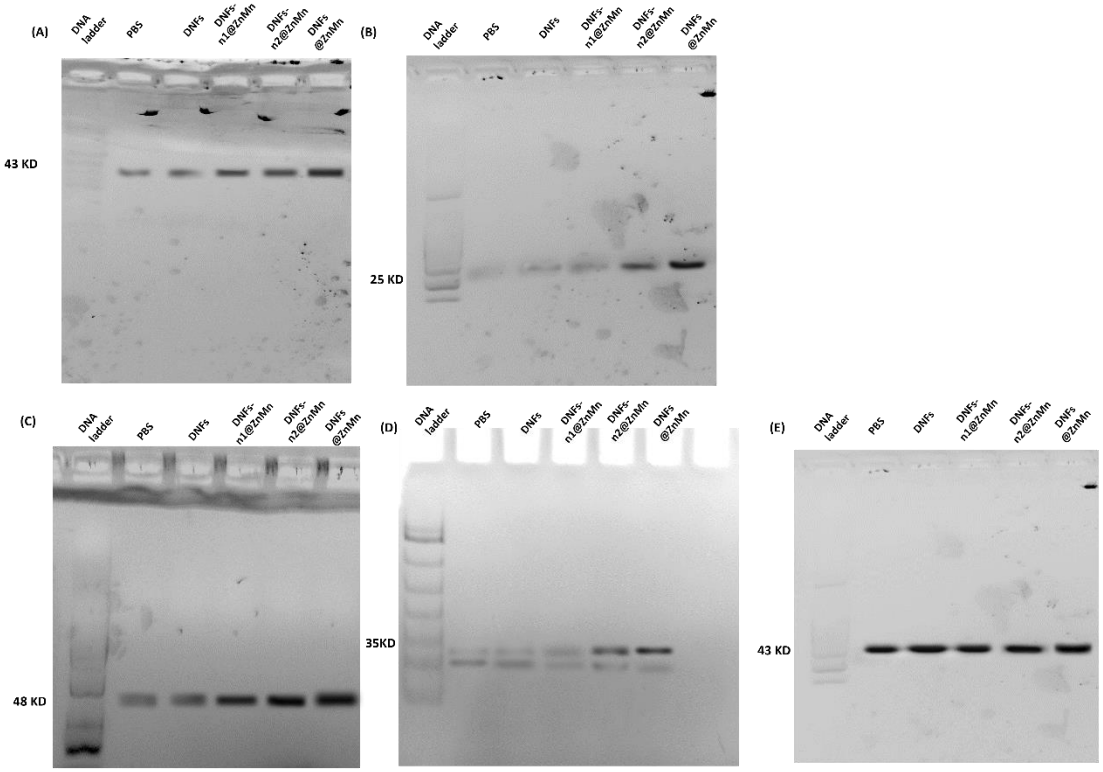

Fig. S37 Western blotting assay to indicate the therapy performance. (A) The intracellular Caspase-1 proteins. (B) The intracellular cleaved-Caspase 1, proteins. (C) The intracellular GSDMD proteins. (D) The intracellular N-GSDMD proteins. (E) Control: β-Actin.

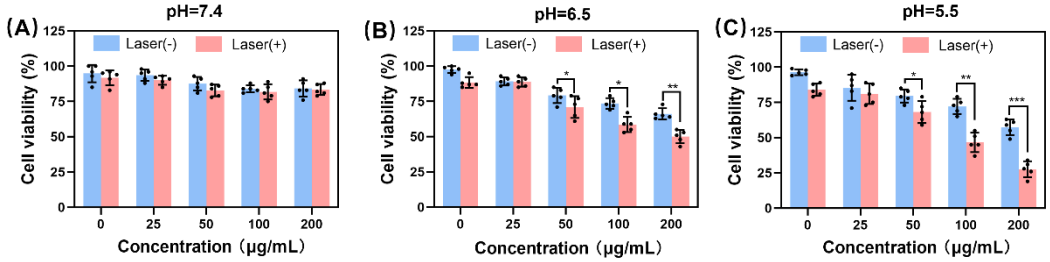

Fig. S38 MTT assay of HeLa cells treated with Ca@DNA-MF at different pH conditions. (A) pH 7.4. (B) pH 6.5. (C) pH 5.5.

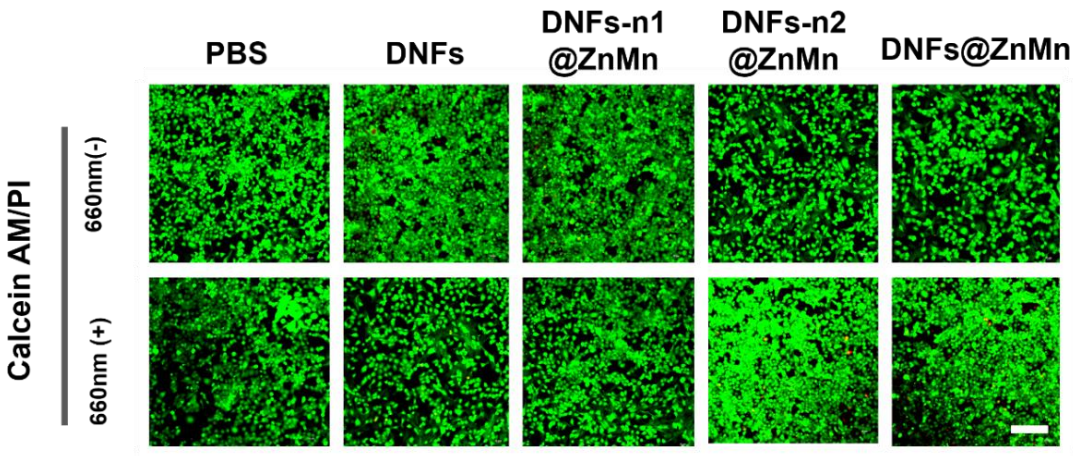

Fig. S39 CLSM images of HeLa cells upon different treatments and stained with Calcein-AM/PI under Laser (-) / Laser (+); Scale bars: 100 μm.

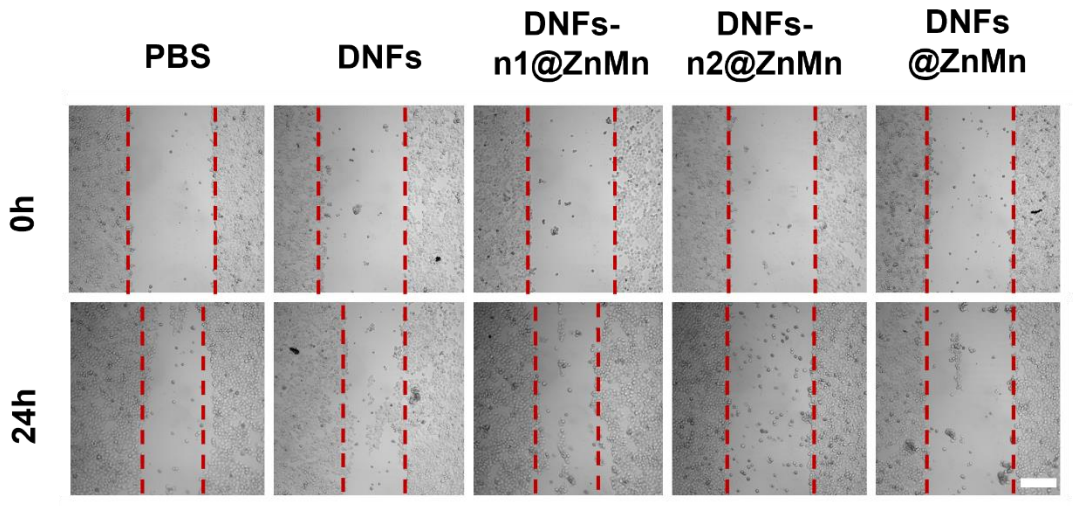

Fig. S40 Images of wound healing assays pre-treated with PBS, DNFs, DNFs-n1@ZnMn, DNFs-n2@ZnMn and DNFs@ZnMn for 24 h. Scale bars: 100 μm.

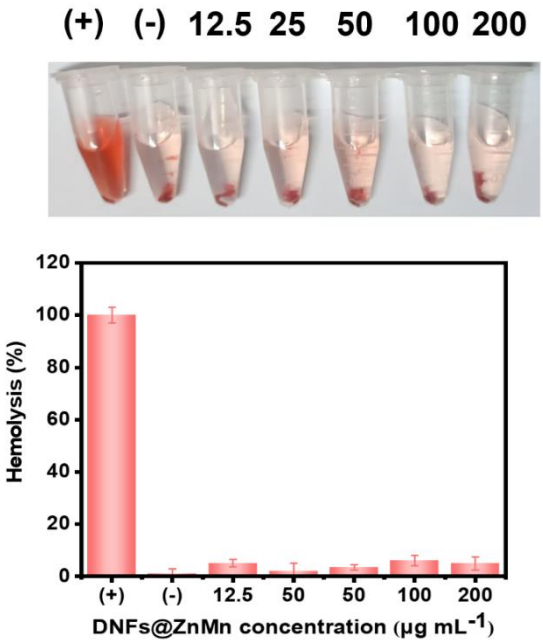

Fig. S41 Hemolysis test for DNFs@ZnMn at different concentrations.

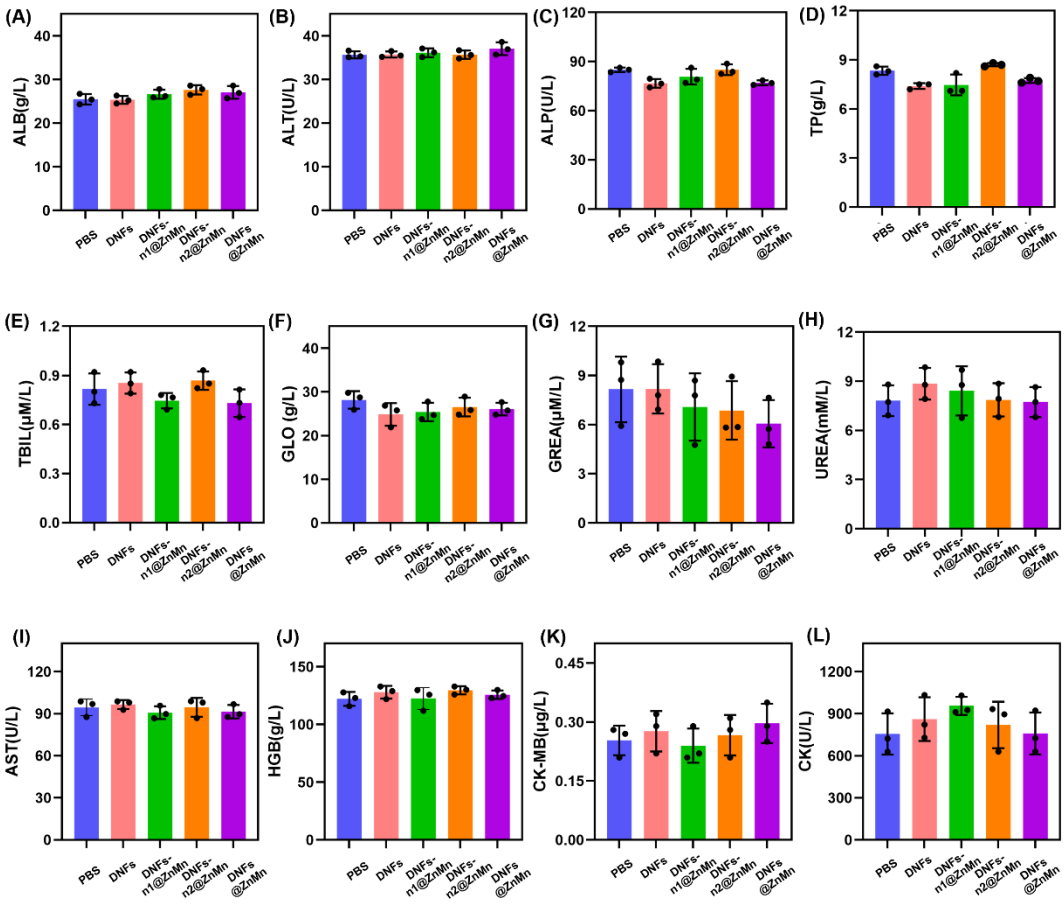

Fig. S42 Serum Biochemical analysis of tumor-bearing mice with different treatments for 14 days. The investigated blood biochemical markers included (A) albumin (ALB), (B) alanine transferase (ALT), (C) alkaline phosphatase (ALP), (D) total protein (TP), (E) total bilirubin (TBIL), (F) globulin (GLO), (G) creatinine (CREA), (H) urea (UREA), (I) aspartate aminotransferase (AST), (J) hemoglobin (HGB), (K) creatine kinase (CK), (L) creatine kinase MB (CK-MB). The TP, TBIL, ALB, GLO, ALP, ALT and AST are liver function related markers; LDH, CK and CK-MB are heart tissue function index; CREA and UREA are renal function index. The mice were divided into five groups: PBS, DNFs, DNF-n1@ZnMn, DNFs-n2@ZnMn, DNFs@ZnMn. Results were presented as mean ± S.D. (n=3).

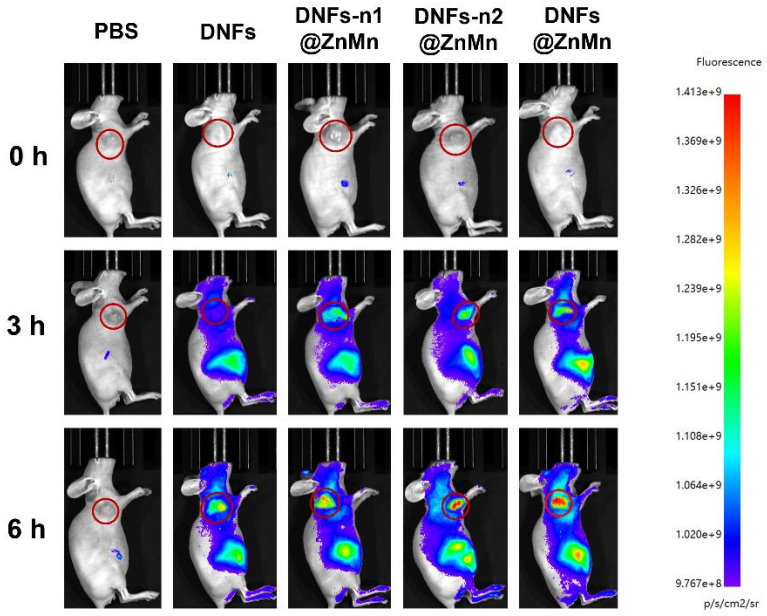

Fig. S43 *In vivo* biodistributions of Cy5-labelled DNFs, DNFs-n1@ZnMn, DNFs-n2@ZnMn and DNFs@ZnMn respectively monitored by live animal imaging after intravenously injection of different formulations of materials to the HeLa tumor-bearing mice.

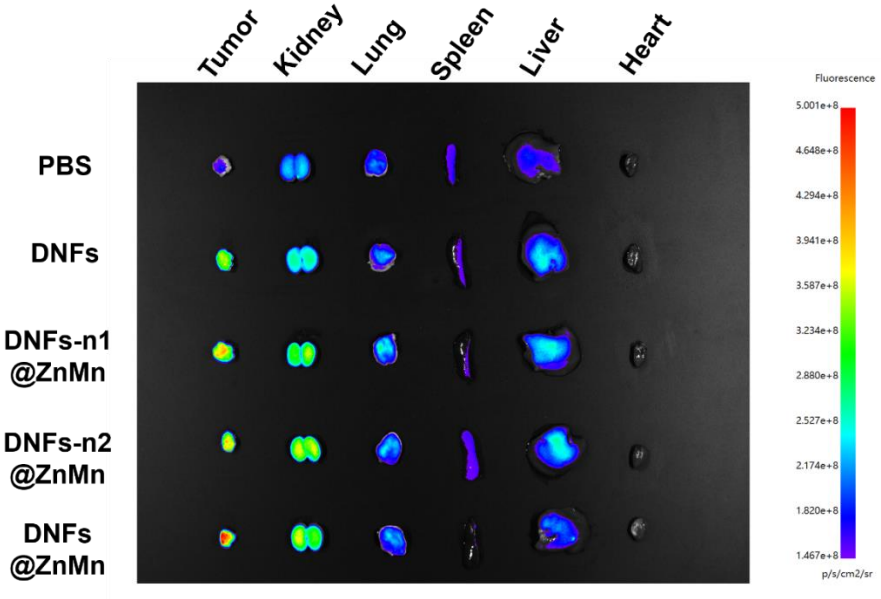

Fig. S44 Fluorescent images of tissues obtained from the mice, which were treated with PBS, DNFs, DNFs-n1@ZnMn, DNFs-n2@ZnMn and DNFs@ZnMn, respectively.

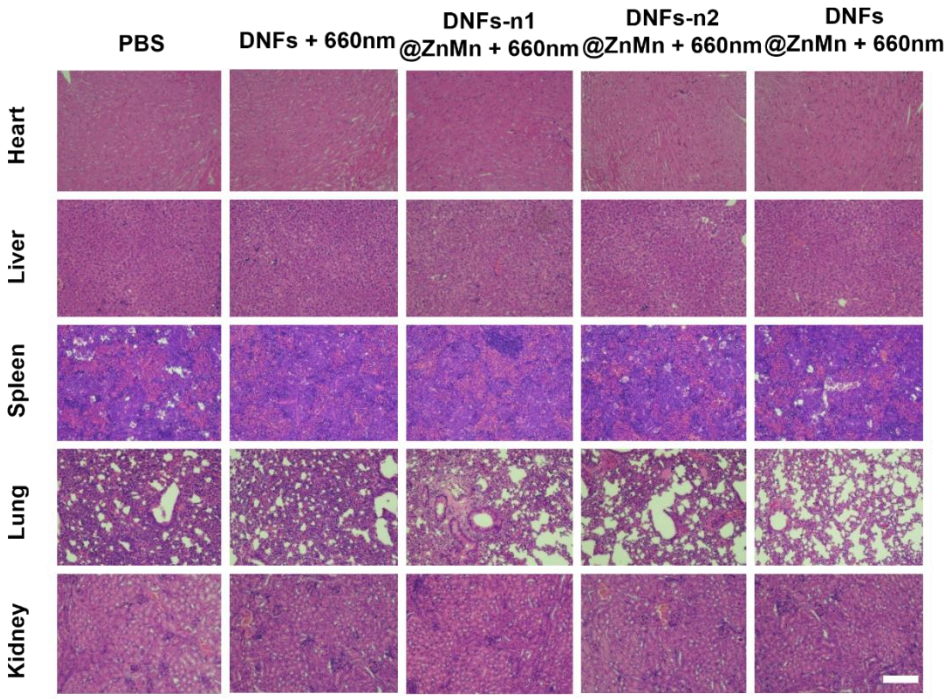

Fig. S45 Hematoxylin-eosin (H&E) staining of the major organs derived from the HeLa tumor-bearing mice at the end of treatment. The heart, liver, spleen, lung, and kidney tissue slices were from tumor-bearing mice with PBS, DNFs, DNFs-n1@ZnMn, DNFs-n2@ZnMn and DNFs@ZnMn treatments for 14 days. Scale bars: 100 μm.

Table S1. DNA and RNA sequences used in this work.

Name	Sequence (5′ To 3′)	Notes
Template-ND	AACTAGATACCAGCTGGTATCCAACTTCGTCTAACAACA ACTCTGGTCGTTGTAG**C**TAGCCTGGGATTGCAAACCAC CACCACCAACACCACCACCACCGTTAGACAGCTC	Non-DNA substrate DNAzyme DNA sequence
Primer-ND	ATACCAGCTGGTATCTAGTT GAGCTGTCTA	/
Template-NR	AACTAGATACCAGCTGGTATCCTTCAACGTCTAACAACA ACTCTGGTCGTTGTAG**G**TAGCCTGGGATTGCAAACCAC CACCACCAACACCACCACCACCGTTAGACAGCTC	Non-ATG5 DNAzyme DNA sequence
Primer-NR	ATACCAGCTGGTATCTAGTT GAGCTGTCTA	/
Template-nApt	AACTAGATACCAGCTGGTATCCTTCAACGTCTAACAACA ACTCTGGTCGTTGTAG**C**TAGCCTGGGATTGCAAAAAAA AAAAAAAAAAAAAAAAAAAACTAGACAGCTC	Non-AS1411 Aptamer DNA sequence
Primer-nApt	ATACCAGCTGGTATCTAGTT GAGCTGTCTA	/
Template-Apt	AACTAGATACCAGCTGGTATCCTTCAACGTCTAACAACA ACTCTGGTCGTTGTAG**C**TAGCCTGGGATTGCAAACCAC CACCACCAACACCACCACCACCGTTAGACAGCTC	ATG5 DNAzyme DNA sequence
Primer-Apt	ATACCAGCTGGTATCTAGTT GAGCTGTCTA	/
DNAzyme	TGCAATCCCAGGCTAGCTACAACGACCAGAGTTG	/
ATG5 Substrate	AAGATCACAAGCAACTCTGG/rA/rU/GGGATTGCAAAA TGACAG	mRNA mimics

Underlined: Complementary to aptamer sequence; Orange letters: Complementary to DNAzyme sequence; Green letters: Complementary to substrate sequence; Red letters: mutant bases.

REFERENCES

[1] J. P. Wang, C. Qu, X. Y. Shao, G. Q.Song, J. Sun, D. H. Shi, R. Jia, H. L. An, H. J. Wang, *Bioactive Materials*, **2023**, *20*, 404 - 417.